A CONVERGENT IMPLICIT DISCRETIZATION OF THE MAXWELL-LANDAU-LIFSHITZ-GILBERT EQUATION

ĽUBOMÍR BAŇAS*, SÖREN BARTELS†, AND ANDREAS PROHL

ABSTRACT. We propose an implicit, fully discrete scheme for the numerical solution of the Landau-Lifshitz-Gilbert equation which is based on linear finite elements and satisfies a discrete sphere constraint as well as a discrete energy law. As numerical parameters tend to zero, solutions weakly accumulate at weak solutions of the Maxwell-Landau-Lifshitz-Gilbert equation. A practical linearization of the nonlinear scheme is proposed and shown to converge for certain scalings of numerical parameters. Computational studies are presented to indicate finite-time blow-up behavior and to study combined electromagnetic phenomena in ferromagnets for benchmark problems.

1. INTRODUCTION

The Maxwell-Landau-Lifschitz-Gilbert equation (MLLG) describes certain electromagnetic phenomena in a ferromagnet occupying the domain $\omega \Subset \Omega \subseteq \mathbb{R}^d$, $d = 2, 3$. For a parameter $\alpha > 0$ which serves as a damping factor, the magnetization field $\mathbf{m} : (0,T) \times \omega \to \mathbb{S}^2$, where $\mathbb{S}^2 = \{\mathbf{x} \in \mathbb{R}^3 | \, |\mathbf{x}| = 1\}$ is the unit sphere, and the electric and magnetic fields $(\mathbf{E}, \mathbf{H}) : (0,T) \times \Omega \to \mathbb{R}^3$ satisfy for all $T > 0$

$$\mathbf{m}_t + \alpha\, \mathbf{m} \times \mathbf{m}_t = (1+\alpha^2)\, \mathbf{m} \times \mathbf{H}_{\text{eff}} \quad \text{in} \quad \omega_T := (0,T) \times \omega\,, \tag{1.1}$$

$$\varepsilon_0\, \mathbf{E}_t - \nabla \times \mathbf{H} + \sigma\, \chi_\omega \mathbf{E} = -\mathbf{J} \quad \text{in} \quad \Omega_T := (0,T) \times \Omega\,, \tag{1.2}$$

$$\mu_0\, \mathbf{H}_t + \nabla \times \mathbf{E} = -\mu_0\, \mathbf{m}_t \qquad \text{in} \quad \Omega_T\,, \tag{1.3}$$

for the (simplified) effective field $\mathbf{H}_{\text{eff}} = \Delta \mathbf{m} + \mathbf{H}$. This choice of $\mathbf{H}_{\text{eff}}$ comprises the most relevant contributions to the more general version (5.1) below. The constants $\varepsilon_0, \mu_0 \geq 0$ denote respectively the electric and magnetic permeability of free space while $\sigma \geq 0$ describes the conductivity of the ferromagnet. The field $\mathbf{J} : \Omega_T \to \mathbb{R}^3$ denotes an applied current density and $\chi_\omega : \Omega \to \{0,1\}$ is the characteristic function of ω. For simplicity we suppose that $\Omega \subset \mathbb{R}^3$ is a bounded cavity with a perfectly conducting outer surface $\partial\Omega$ into which the ferromagnet $\omega \Subset \Omega$ is embedded, and $\Omega \setminus \overline{\omega}$ is assumed to be vacuum [14]. The system (1.1)–(1.3) is supplemented with initial conditions

$$\mathbf{m}(0,\cdot) = \mathbf{m}_0 \quad \text{in}\ \omega\,, \qquad \mathbf{E}(0,\cdot) = \mathbf{E}_0\,, \quad \mathbf{H}(0,\cdot) = \mathbf{H}_0 \quad \text{in}\ \Omega \tag{1.4}$$

and boundary conditions

$$\partial_{\mathbf{n}} \mathbf{m} = 0 \quad \text{on}\ \partial\omega_T\,, \qquad \mathbf{E} \times \mathbf{n} = 0 \quad \text{on}\ \partial\Omega_T\,. \tag{1.5}$$

We remark that the inclusion of a damping term is necessary to permit the magnetic field to align with the effective field and refer the reader to [5, 23, 11] for a more detailed discussion of the mathematical model. Interesting computational studies of the model (1.1)–(1.5) can be found in [14, 21].

1991 *Mathematics Subject Classification.* 35K55, 65M12, 65M15, 68U10, 94A08.

Key words and phrases. ferromagnetism, Maxwell-Landau-Lifshitz-Gilbert equation, finite elements, convergence.

*Supported by the EPSRC grant EP/C548973/1.

†Supported by Deutsche Forschungsgemeinschaft through the DFG Research Center MATHEON 'Mathematics for key technologies' in Berlin

The construction of convergent numerical schemes for the Maxwell-Landau-Lifshitz-Gilbert system (1.1)–(1.5) is difficult due to the nonlinear character of (1.1). Moreover, the limited flexibility of piecewise polynomial finite elements and the artificial damping of implicit time-discretization schemes make it hard to appropriately account for the constraint $|\mathbf{m}| = 1$ a.e. in ω_T. The semi-discrete scheme proposed in [14] uses numerical integration to guarantee that the constraint is satisfied at the nodes of a triangulation. Stability of that scheme is proved in [14] but its convergence has not been discussed in the literature so far.

According to Landau & Lifshitz [10], damped precession ($\alpha > 0$) of the magnetization $\mathbf{m} : \omega_T \to \mathbb{S}^2$ is governed by

$$\mathbf{m}_t = \mathbf{m} \times \mathbf{H}_{\text{eff}} - \alpha\, \mathbf{m} \times (\mathbf{m} \times \mathbf{H}_{\text{eff}})\,. \tag{1.6}$$

Gilbert's approach modifies the undamped precession equation by a damping term which is proportional to the rate of change of magnetization, see (1.1). Both approaches are analytically equivalent for smooth magnetization fields and weak solutions to (MLLG) exist in both cases [23, 6]. The numerical analysis differs significantly and Gilbert's approach turns out attractive from a numerical viewpoint. Explicit and implicit discretizations for the simplest choice $\mathbf{H}_{\text{eff}} = \Delta\mathbf{m}$ have been proposed and analyzed in [2, 4, 3] and approximations are known to respectively converge conditionally and unconditionally with respect to discretization parameters to weak solutions of (1.1). Corresponding results for (1.6) are so far only available for (locally existing) strong solutions, cf. [18, 7]. The articles [13, 20] study convergence for the simplification $\mathbf{H}_{\text{eff}} = \mathbf{H}$ for cases where smooth solutions to (1.1)–(1.5) exist. Convergence of iterates of the following scheme to weak solutions of (1.1) for $\mathbf{H}_{\text{eff}} = \Delta\mathbf{m}$ is verified in [3]; the proof relies on conservation of $|\mathbf{m}_h^j| = 1$ at all mesh points and for all $j \geq 0$ as well as a discrete energy law.

Algorithm 1.1. *Let $\mathbf{m}_h^0 \in \mathbf{V}_h$. Given $j \geq 0$ and $\mathbf{m}_h^j \in \mathbf{V}_h$, let $\mathbf{m}_h^{j+1} \in \mathbf{V}_h$ solve*

$$(d_t\mathbf{m}_h^{j+1}, \boldsymbol{\phi}_h)_h + \alpha\, (\mathbf{m}_h^j \times d_t\mathbf{m}_h^{j+1}, \boldsymbol{\phi}_h)_h = (1+\alpha^2)(\overline{\mathbf{m}}_h^{j+1/2} \times \tilde{\Delta}_h \overline{\mathbf{m}}_h^{j+1/2}, \boldsymbol{\phi}_h)_h \quad \forall \boldsymbol{\phi}_h \in \mathbf{V}_h\,.$$

Here, $\mathbf{V}_h \subset W^{1,2}(\omega;\mathbb{R}^3)$ is the finite element space subordinate to a triangulation $\mathcal{T}_h$ of ω consisting of piecewise linear functions and $(\cdot,\cdot)_h$ denotes a discrete version (numerical integration) of the inner product in $L^2(\omega;\mathbb{R}^3)$. Moreover, $\tilde{\Delta}_h : W^{1,2}(\omega;\mathbb{R}^3) \to \mathbf{V}_h$ is an approximation of the Laplace operator. For a time step size $k > 0$ we write $d_t\varphi^j := k^{-1}\big(\varphi^j - \varphi^{j-1}\big)$ for $j \geq 1$, and $\overline{\varphi}^{j+1/2} := \frac{1}{2}\big(\varphi^{j+1} + \varphi^j\big)$ for $j \geq 0$ and a sequence $\{\varphi^j\}_{j\geq 0}$; we refer the reader to Section 2 for details.

The goal of this work is (i) to propose a discretization of (1.1)–(1.3) based on linear finite elements which satisfies a discrete sphere constraint and a discrete energy identity, (ii) to verify convergence of iterates towards a weak solution of (1.1)–(1.3), and (iii) to propose a reliable solver for the nonlinear system of equations in each time step. This program is motivated by possible finite-time blow-up behaviour of solutions to (1.1)–(1.3), see Section 5, whose numerical simulation requires reliable numerical schemes. Our strategy is to appropriately modify Algorithm 1.1 and to extend its analysis from [3].

The discretization of (1.1)–(1.3) requires a proper choice of Ansatz spaces for the approximation of $(\mathbf{E}, \mathbf{H})$. Suitable pairs can be found in [13, 14] and we let $\mathbf{X}_h \subset \mathbf{H}_0(\mathbf{curl};\Omega)$ and $\mathbf{Y}_h \subset L^2(\Omega,\mathbb{R}^3)$ be finite dimensional spaces satisfying $\nabla \times \mathbf{X}_h \subset \mathbf{Y}_h$. We then aim at analyzing the following algorithm for the numerical approximation of (MLLG).

Algorithm 1.2. *Let* $(\mathbf{m}_h^0, \mathbf{E}_h^0, \mathbf{H}_h^0) \in \mathbf{V}_h \times \mathbf{X}_h \times \mathbf{Y}_h$. *For* $j \geq 0$ *and* $(\mathbf{m}_h^j, \mathbf{E}_h^j, \mathbf{H}_h^j) \in \mathbf{V}_h \times \mathbf{X}_h \times \mathbf{Y}_h$, *let* $(\mathbf{m}_h^{j+1}, \mathbf{E}_h^{j+1}, \mathbf{H}_h^{j+1}) \in \mathbf{V}_h \times \mathbf{X}_h \times \mathbf{Y}_h$ *solve*

$$(1.7)\qquad \begin{aligned}&(d_t\mathbf{m}_h^{j+1}, \boldsymbol{\phi}_h)_h + \alpha\,(\mathbf{m}_h^j \times d_t\mathbf{m}_h^{j+1}, \boldsymbol{\phi}_h)_h \\ &\qquad = (1+\alpha^2)\Big(\overline{\mathbf{m}}_h^{j+1/2} \times (\tilde{\Delta}_h \overline{\mathbf{m}}_h^{j+1/2} + \mathbf{P}_{\mathbf{V}_h}\overline{\mathbf{H}}_h^{j+1/2}), \boldsymbol{\phi}_h\Big)_h \qquad \forall\, \boldsymbol{\phi}_h \in \mathbf{V}_h\,,\end{aligned}$$

$$(1.8)\qquad \varepsilon_0\,(d_t\mathbf{E}_h^{j+1}, \boldsymbol{\varphi}_h) - (\overline{\mathbf{H}}_h^{j+1/2}, \nabla\times\boldsymbol{\varphi}_h) + \sigma\,(\chi_\omega \overline{\mathbf{E}}_h^{j+1/2}, \boldsymbol{\varphi}_h) = -(\overline{\mathbf{J}}_h^{j+1/2}, \boldsymbol{\varphi}_h) \qquad \forall\boldsymbol{\varphi}_h \in \mathbf{X}_h\,,$$

$$(1.9)\qquad \mu_0\,(d_t\mathbf{H}_h^{j+1}, \boldsymbol{\mathfrak{z}}_h) + (\nabla\times\overline{\mathbf{E}}_h^{j+1/2}, \boldsymbol{\mathfrak{z}}_h) = -\mu_0\,(d_t\mathbf{m}_h^{j+1}, \boldsymbol{\mathfrak{z}}_h) \qquad \forall\boldsymbol{\mathfrak{z}}_h \in \mathbf{Y}_h\,.$$

Here, $\mathbf{P}_{\mathbf{V}_h} : L^2(\omega,\mathbb{R}^3) \to \mathbf{V}_h$, with $(\mathbf{P}_{\mathbf{V}_h}\mathbf{u}, \boldsymbol{\varphi}_h)_h = (\mathbf{u}, \boldsymbol{\varphi}_h)$ for all $\boldsymbol{\varphi}_h \in \mathbf{V}_h$ denotes the L^2-projection into $\mathbf{V}_h$.

Lemma 3.1 below establishes conservation of $|\,\mathbf{m}_h^j\,| = 1$, $j \geq 0$, at nodes of the triangulation $\mathcal{T}_h$, and a discrete energy law for solutions to Algorithm 1.2. Our first main result is Theorem 3.1 which states unconditional convergence of subsequences of outputs of Algorithm 1.2. A simple fixed-point iteration for the approximate solution of the nonlinear system of equations in each step of Algorithm 1.2 which preserves the unit-length constraint is proposed in Algorithm 4.1. Its convergence is proved under the mesh constraint $k = \mathcal{O}(h^2)$ in Lemma 4.1. Numerical studies which indicate possible finite-time blow-up of weak solutions of (1.1)–(1.5) are reported in Section 5. Simulations of benchmark problems from [16] are also reported.

2. Preliminaries

Throughout this paper we assume that $\mathcal{T}_h$ is a regular triangulation of the polygonal or polyhedral bounded Lipschitz domain $\Omega \subset \mathbb{R}^d$ into triangles or tetrahedra of maximal mesh-size (maximal diameter of triangles or tetrahedra) $h > 0$ for $d = 2$ or $d = 3$, respectively, and $\mathcal{T}_h\big|_\omega$ denotes its restriction to $\omega \Subset \Omega$. We define the lowest order conforming finite element space $\mathbf{V}_h \subset W^{1,2}(\omega;\mathbb{R}^3)$ by

$$\mathbf{V}_h = \big\{\boldsymbol{\phi}_h \in C(\overline{\omega};\mathbb{R}^3) : \boldsymbol{\phi}_h|_K \in \mathcal{P}_1(K;\mathbb{R}^3) \quad \forall\, K \in \mathcal{T}_h\big|_\omega\big\}\,,$$

where $\mathcal{P}_1(K;\mathbb{R}^3)$ denotes the set of polynomials of total degree less or equal to one if restricted to the element $K \in \mathcal{T}_h$. Given the set of nodes $\{\mathbf{x}_\ell : \ell \in L\}$ of the triangulation $\mathcal{T}_h\big|_\omega$, the nodal interpolation operator $\boldsymbol{\mathcal{I}}_{\mathbf{V}_h} : C(\overline{\omega};\mathbb{R}^3) \to \mathbf{V}_h$ satisfies $\boldsymbol{\mathcal{I}}_{\mathbf{V}_h}\boldsymbol{\phi}(\mathbf{x}_\ell) = \boldsymbol{\phi}(\mathbf{x}_\ell)$ for all $\ell \in L$. We let $\langle\cdot,\cdot\rangle$ denote the inner product in $\mathbb{R}^d$ and we define

$$\big(\mathbf{f},\mathbf{g}\big) = \int_\Omega \langle\mathbf{f},\mathbf{g}\rangle\,\mathrm{d}\mathbf{x} \qquad \text{and} \qquad \big(\boldsymbol{\phi},\boldsymbol{\mathfrak{z}}\big)_h = \int_\omega \boldsymbol{\mathcal{I}}_{\mathbf{V_h}}\big(\langle\boldsymbol{\phi},\boldsymbol{\mathfrak{z}}\rangle\big)\,\mathrm{d}\mathbf{x} = \sum_{\ell\in L}\beta_\ell\langle\boldsymbol{\phi}(\mathbf{x}_\ell),\boldsymbol{\mathfrak{z}}(\mathbf{x}_\ell)\rangle\,,$$

for $\mathbf{f},\mathbf{g} \in L^2(\Omega;\mathbb{R}^d)$, certain weights $\beta_\ell > 0$, $\ell \in L$, and continuous functions $\boldsymbol{\phi}, \boldsymbol{\mathfrak{z}} \in C(\overline{\omega};\mathbb{R}^3)$. Note that we use the notation $(\cdot,\cdot)$ for the inner product in $L^2(\Omega)$ as well as in $L^2(\omega)$ – it will always be clear from the context which of them it represents. For each $\ell \in L$ we let $\varphi_\ell \in C(\overline{\omega})$ denote the nodal basis function in $\mathbf{V}_h$ which is $\mathcal{T}_h$-elementwise affine and satisfies $\varphi_\ell(\mathbf{x}_m) = \delta_{\ell m}$ for all $m, \ell \in L$ and we define $\beta_\ell = \int_\omega \varphi_\ell\,\mathrm{d}\mathbf{x}$. We write $||\boldsymbol{\phi}||_h^2 = \big(\boldsymbol{\phi},\,\boldsymbol{\phi}\big)_h$ and notice that

$$(2.1)\qquad \|\,\boldsymbol{\phi}_h\,\|_{L^2}^2 \leq \|\,\boldsymbol{\phi}_h\,\|_h^2 \leq (d+2)\,\|\,\boldsymbol{\phi}_h\,\|_{L^2}^2 \qquad \forall\boldsymbol{\phi}_h \in \mathbf{V}_h\,.$$

Basic interpolation estimates yield for all $\boldsymbol{\phi}_h, \boldsymbol{\mathfrak{z}}_h \in \mathbf{V}_h$ that

$$(2.2)\qquad \big|(\boldsymbol{\phi}_h,\boldsymbol{\mathfrak{z}}_h)_h - (\boldsymbol{\phi}_h,\boldsymbol{\mathfrak{z}}_h)\big| \leq Ch\|\boldsymbol{\phi}_h\|\,\|\nabla\boldsymbol{\mathfrak{z}}_h\|\,.$$

We define a discrete Laplace operator $\tilde{\Delta}_h : W^{1,2}(\omega;\mathbb{R}^3) \to \mathbf{V}_h$ by

$$(2.3)\qquad (-\tilde{\Delta}_h\boldsymbol{\phi}, \boldsymbol{\chi}_h)_h = (\nabla\boldsymbol{\phi}, \nabla\boldsymbol{\chi}_h) \quad \forall\boldsymbol{\chi}_h \in \mathbf{V}_h\,.$$

It is well-known that there exist constants $c_1, c_2 > 0$ such that for all $\boldsymbol{\phi}_h \in \mathbf{V}_h$ and all $\ell \in L$ we have, see, e.g., [3],

$$||\tilde{\Delta}_h \boldsymbol{\phi}_h||_h \leq c_1 h_{min}^{-1} ||\nabla \boldsymbol{\phi}_h||_{L^2} \leq c_2 h_{min}^{-2} ||\boldsymbol{\phi}_h||_{L^2}\,, \tag{2.4}$$

$$|\tilde{\Delta}_h \boldsymbol{\phi}_h(\mathbf{x}_\ell)| \leq c_3 h_{min}^{-2} ||\boldsymbol{\phi}_h||_{L^\infty}\,, \tag{2.5}$$

where $h_{\min} > 0$ is the minimal diameter of elements in $\mathcal{T}_h$.

To discretize Maxwell's equations, we employ finite element spaces $\mathbf{X}_h \subset \mathbf{H}_0(\mathbf{curl};\Omega)$, $\mathbf{Y}_h \subset L^2(\Omega;\mathbb{R}^3)$ subordinate to $\mathcal{T}_h$ such that $\nabla \times \mathbf{X}_h \subset \mathbf{Y}_h$; common examples are Nédélec's first and second family of edge elements on tetrahedra, where we choose the latter subsequently; cf. [12, Chapter 8,5],

$$\mathbf{X}_h = \left\{ \boldsymbol{\varphi}_h \in \mathbf{H}_0(\mathbf{curl};\Omega) : \boldsymbol{\varphi}_h|_K \in \mathcal{P}_1(K;\mathbb{R}^3) \quad \forall\, K \in \mathcal{T}_h \right\},$$

and

$$\mathbf{Y}_h = \left\{ \boldsymbol{\zeta}_h \in L^2(\Omega;\mathbb{R}^3) : \boldsymbol{\zeta}_h|_K \in \mathcal{P}_0(K;\mathbb{R}^3) \quad \forall\, K \in \mathcal{T}_h \right\},$$

where global interpolants of sufficiently smooth functions ($\delta > 0$, $p > 2$)

$$\boldsymbol{\mathcal{I}}_{\mathbf{X}_h} : W^{1/2+\delta,2}(\Omega,\mathbb{R}^3) \cap W^{1,p}(\Omega,\mathbb{R}^3) \to \mathbf{X}_h\,, \quad \text{and} \quad \boldsymbol{\mathcal{I}}_{\mathbf{Y}_h} : W^{1/2+\delta,2}(\Omega,\mathbb{R}^3) \to \mathbf{Y}_h$$

exist and satisfy [12, Theorem 8.15, Remark 8.8]

$$\|\, \boldsymbol{\varphi} - \boldsymbol{\mathcal{I}}_{\mathbf{X}_h}\boldsymbol{\varphi} \,\|_{L^2} + h \,\|\, \nabla \times (\boldsymbol{\varphi} - \boldsymbol{\mathcal{I}}_{\mathbf{X}_h}\boldsymbol{\varphi}) \,\|_{L^2} \leq C h^2 \,\|\, \nabla^2 \boldsymbol{\varphi} \,\|_{L^2}\,, \tag{2.6}$$

$$\|\, \boldsymbol{\zeta} - \boldsymbol{\mathcal{I}}_{\mathbf{Y}_h}\boldsymbol{\zeta} \,\|_{L^2} \leq C h \,\|\, \boldsymbol{\zeta} \,\|_{H^1} \tag{2.7}$$

for all $\boldsymbol{\varphi} \in W^{2,2}(\Omega,\mathbb{R}^3)$ and $\boldsymbol{\zeta} \in W^{1,2}(\Omega,\mathbb{R}^3)$.

To define weak solutions of (1.1)–(1.3), we assume that the given data satisfy

$$\mathbf{m}_0 \in W^{1,2}(\omega,\mathbb{S}^2)\,, \quad \mathbf{H}_0,\, \mathbf{E}_0 \in L^2(\Omega,\mathbb{R}^3)\,, \quad \mathbf{J} \in L^2(\Omega_T,\mathbb{R}^3)\,. \tag{2.8}$$

We assume that the set of initial data satisfies $\operatorname{div} \mathbf{H}_0 = 0$ and is consistent in the sense that

$$\operatorname{div}(\mathbf{H}_0 + \chi_\omega \mathbf{m}_0) = 0 \quad \text{in } \Omega\,, \qquad \langle \mathbf{H}_0 + \chi_\omega \mathbf{m}_0, \mathbf{n} \rangle = 0 \quad \text{on } \partial\Omega\,. \tag{2.9}$$

Definition 2.1. *Suppose* (2.8)–(2.9)*. Then* $(\,\mathbf{m},\mathbf{E},\mathbf{H}\,)$ *is called a weak solution to (MLLG), if for all* $T > 0$*,*

1. $\mathbf{m} \in L^\infty\big(0,T;W^{1,2}(\omega,\mathbb{R}^3)\big)$*, such that* $\mathbf{m}_t \in L^2(\omega_T,\mathbb{R}^3)$ *and* $|\,\mathbf{m}\,| = 1$ *a.e. in* ω_T*, and* $\mathbf{E},\mathbf{H} \in L^\infty\big(0,T;L^2(\Omega,\mathbb{R}^3)\big)$*;*
2. *for all* $\boldsymbol{\phi} \in C^\infty\big(\overline{\omega_T};\mathbb{R}^3)\big)$*, and* $\boldsymbol{\zeta} \in \mathcal{D}\big([0,T);C^\infty(\Omega,\mathbb{R}^3) \cap \mathbf{H}_0(\mathbf{curl},\Omega)\big)$*,*

$$\begin{aligned}\int_{\omega_T} \langle \mathbf{m}_t, \boldsymbol{\phi} \rangle \,\mathrm{d}\mathbf{x}\,\mathrm{d}t &+ \alpha \int_{\omega_T} \langle \mathbf{m} \times \mathbf{m}_t, \boldsymbol{\phi} \rangle \,\mathrm{d}\mathbf{x}\,\mathrm{d}t \\ &= -(1+\alpha^2)\Big[\int_{\omega_T} \langle \mathbf{m} \times \nabla \mathbf{m}, \nabla \boldsymbol{\phi} \rangle \,\mathrm{d}\mathbf{x}\,\mathrm{d}t - \int_{\omega_T} \langle \mathbf{m} \times \mathbf{H}, \boldsymbol{\phi} \rangle \,\mathrm{d}\mathbf{x}\,\mathrm{d}t\Big]\,,\end{aligned} \tag{2.10}$$

$$\begin{aligned}-\varepsilon_0 \int_{\Omega_T} \langle \mathbf{E}, \boldsymbol{\zeta}_t \rangle \,\mathrm{d}\mathbf{x}\,\mathrm{d}t &- \int_{\Omega_T} \langle \mathbf{H}, \nabla \times \boldsymbol{\zeta} \rangle \,\mathrm{d}\mathbf{x}\,\mathrm{d}t \\ &+\sigma \int_{\omega_T} \langle \mathbf{E}, \boldsymbol{\zeta} \rangle \,\mathrm{d}\mathbf{x}\,\mathrm{d}t = -\int_{\Omega_T} \langle \mathbf{J}, \boldsymbol{\zeta} \rangle \,\mathrm{d}\mathbf{x}\,\mathrm{d}t + \varepsilon_0 \int_\Omega \langle \mathbf{E}_0, \boldsymbol{\zeta}(0,\cdot) \rangle \,\mathrm{d}\mathbf{x}\,,\end{aligned} \tag{2.11}$$

$$\begin{aligned}-\mu_0 \int_{\Omega_T} \langle \mathbf{H} + \chi_\omega \mathbf{m}, \boldsymbol{\zeta}_t \rangle \,\mathrm{d}\mathbf{x}\,\mathrm{d}t &+ \int_{\Omega_T} \langle \mathbf{E}, \nabla \times \boldsymbol{\zeta} \rangle \,\mathrm{d}\mathbf{x}\,\mathrm{d}t \\ &= \mu_0 \int_\Omega \langle \mathbf{H}_0, \boldsymbol{\zeta}(0,\cdot) \rangle \,\mathrm{d}\mathbf{x} + \mu_0 \int_\omega \langle \mathbf{m}_0, \boldsymbol{\zeta}(0,\cdot) \rangle \,\mathrm{d}\mathbf{x}\,;\end{aligned} \tag{2.12}$$

3. *we have* $\mathbf{m}(0,\cdot) = \mathbf{m}_0$ *in the sense of traces;*

(4) *for almost all $T' \in (0,T)$ we have*

$$\mathcal{E}_{(\mathbf{m},\mathbf{H},\mathbf{E})}(T') + \int_{\omega_{T'}} \big(\frac{\alpha\mu_0}{1+\alpha^2}\,|\,\mathbf{m}_t\,|^2 + \sigma|\,\mathbf{E}\,|^2\big)\,\mathrm{d}\mathbf{x}\,\mathrm{d}t \le \mathcal{E}_{(\mathbf{m},\mathbf{H},\mathbf{E})}(0) - \int_{\Omega_{T'}} (\mathbf{J},\mathbf{E})\,\mathrm{d}\mathbf{x}\,\mathrm{d}t\,,$$

where

$$\mathcal{E}_{(\mathbf{m},\mathbf{H},\mathbf{E})}(T') = \frac{\mu_0}{2}\int_\omega |\,\nabla\mathbf{m}(T',\cdot)\,|^2\,\mathrm{d}\mathbf{x} + \int_\Omega \Big[\frac{\mu_0}{2}|\,\mathbf{H}(T',\cdot)\,|^2 + \frac{\varepsilon_0}{2}|\,\mathbf{E}(T',\cdot)\,|^2\Big]\,\mathrm{d}\mathbf{x}\,.$$

Existence of weak solutions has first been shown in [6].

3. Stability and Convergence

The following lemma provides a discrete counterpart of (4) in Definition 2.1 for Algorithm 1.2. Solvability of (1.7)–(1.9) follows from a contraction argument, which employs (i) discrete energy law (Lemma 3.1), (ii) isomorphism property of the mapping $\mathbf{v} \mapsto \mathbf{v} - \mathbf{u}\times\mathbf{v}$ in $\mathbb{R}^3$ (cf. [1, p. 1079]), and (iii) in particular, isomorphism property for the linear problem (1.8)–(1.9). For a less general proof of existence of a solution, see Section 4.

Lemma 3.1. *Suppose that $|\mathbf{m}_h^0(\mathbf{x}_\ell)| = 1$ for all $\ell \in L$. Then the sequence $\{(\mathbf{m}_h^j,\mathbf{E}_h^j,\mathbf{H}_h^j)\}_{j\ge 0}$ produced by Algorithm 1.2 satisfies for all $j \ge 0$*

$$\text{(i)}\qquad |\,\mathbf{m}_h^{j+1}(\mathbf{x}_\ell)\,| = 1 \quad \forall\,\ell\in L\,,$$

$$\text{(ii)}\qquad \mathcal{E}_h\big(\{\mathbf{m}_h^{j+1},\mathbf{H}_h^{j+1},\mathbf{E}_h^{j+1}\}\big) + k\sum_{\ell=0}^{j}\frac{\alpha\mu_0}{1+\alpha^2}\|\,d_t\mathbf{m}_h^{\ell+1}\,\|_h^2 + \sigma\,\|\,\overline{\mathbf{E}}_h^{\ell+1/2}\,\|_{L^2(\omega)}^2$$

$$= \mathcal{E}_h\big(\{\mathbf{m}_h^0,\mathbf{H}_h^0,\mathbf{E}_h^0\}\big) - k\sum_{\ell=0}^{j}(\overline{\mathbf{J}}_h^{\ell+1/2},\overline{\mathbf{E}}_h^{\ell+1/2})\,,$$

where

$$\mathcal{E}_h\big(\{\mathbf{m}_h^j,\mathbf{H}_h^j,\mathbf{E}_h^j\}\big) = \frac{\mu_0}{2}\int_\omega |\,\nabla\mathbf{m}_h^j\,|^2\,\mathrm{d}\mathbf{x} + \int_\Omega\Big[\frac{\mu_0}{2}\,|\,\mathbf{H}_h^j\,|^2 + \frac{\varepsilon_0}{2}\,|\,\mathbf{E}_h^j\,|^2\Big]\,\mathrm{d}\mathbf{x}\,.$$

Proof. Verification of (i) follows from choosing $\boldsymbol{\phi}_h = \varphi_\ell\overline{\mathbf{m}}_h^{j+1/2}(\mathbf{x}_\ell) \in \mathbf{V}_h$ for $\ell\in L$ in (1.7): with the properties of the discrete inner product and the cross product we infer

$$\beta_\ell d_t\big|\mathbf{m}_h^{j+1}(\mathbf{x}_\ell)\big|^2 = \beta_\ell\langle d_t\mathbf{m}_h^{j+1}(\mathbf{x}_\ell),\overline{\mathbf{m}}_h^{j+1/2}(\mathbf{x}_\ell)\rangle = \big(d_t\mathbf{m}_h^{j+1},\varphi_\ell\overline{\mathbf{m}}_h^{j+1/2}(\mathbf{x}_\ell)\big)_h = 0.$$

Hence, if $\big|\mathbf{m}_h^j(\mathbf{x}_\ell)\big| = 1$ then also $\big|\mathbf{m}_h^{j+1}(\mathbf{x}_\ell)\big| = 1$. To verify (ii), we first choose $\boldsymbol{\phi}_h = -\big(\tilde\Delta_h\overline{\mathbf{m}}_h^{j+1/2} + \mathbf{P}_{\mathbf{V}_h}\overline{\mathbf{H}}_h^{j+1/2}\big)$ to obtain

$$\frac{1}{2}d_t\|\,\nabla\mathbf{m}_h^{j+1}\,\|_{L^2}^2 - (d_t\mathbf{m}_h^{j+1},\mathbf{P}_{\mathbf{V}_h}\overline{\mathbf{H}}_h^{j+1/2})_h = \alpha\big(\overline{\mathbf{m}}_h^{j+1/2}\times d_t\mathbf{m}_h^{j+1},\tilde\Delta_h\overline{\mathbf{m}}_h^{j+1/2} + \mathbf{P}_{\mathbf{V}_h}\overline{\mathbf{H}}_h^{j+1/2}\big)_h\,.$$

Choosing $\boldsymbol{\phi}_h = d_t\mathbf{m}_h^{j+1}$ yields to

$$\frac{\alpha}{1+\alpha^2}\|\,d_t\mathbf{m}_h^{j+1}\,\|_h^2 = \alpha\Big(\overline{\mathbf{m}}_h^{j+1/2}\times(\tilde\Delta_h\overline{\mathbf{m}}_h^{j+1/2} + \mathbf{P}_{\mathbf{V}_h}\overline{\mathbf{H}}_h^{j+1/2}),d_t\mathbf{m}_h^{j+1}\Big)_h\,.$$

Adding the last two identities and using the definition of $\mathbf{P}_{\mathbf{V}_h}$ lead to

$$\frac{1}{2}d_t\|\,\nabla\mathbf{m}_h^{j+1}\,\|_{L^2}^2 + \frac{\alpha}{1+\alpha^2}\|\,d_t\mathbf{m}_h^{j+1}\,\|_h^2 = (d_t\mathbf{m}_h^{j+1},\overline{\mathbf{H}}_h^{j+1/2})\,.$$

In a second step, we choose $(\boldsymbol{\varphi}_h,\mathfrak{Z}_h) = (\overline{\mathbf{E}}_h^{j+1/2},\overline{\mathbf{H}}_h^{j+1/2})$ in (1.8)–(1.9) and add resulting identities,

$$d_t\big(\frac{\mu_0}{2}\,\|\,\mathbf{H}_h^{j+1}\,\|_{L^2}^2 + \frac{\varepsilon_0}{2}\,\|\,\mathbf{E}_h^{j+1}\,\|_{L^2}^2\big) + \sigma\,\|\,\chi_\omega\overline{\mathbf{E}}_h^{j+1/2}\,\|_{L^2}^2 = -\mu_0\,(d_t\mathbf{m}_h^{j+1},\overline{\mathbf{H}}_h^{j+1/2}) - (\overline{\mathbf{J}}_h^{j+1/2},\overline{\mathbf{E}}_h^{j+1/2})\,.$$

Summation of last two identities then proves assertion (ii). ∎

Definition 3.1. *For* $\mathbf{x} \in \Omega$ *and* $t \in [t_j, t_{j+1})$ *define for* $\boldsymbol{\xi}^\ell = \mathbf{m}_h^\ell, \mathbf{H}_h^\ell, \mathbf{E}_h^\ell, \mathbf{J}_h^\ell$*, and* $\ell = j, j+1$,

$$\tilde{\boldsymbol{\xi}}(t,\mathbf{x}) := \frac{t-t_j}{k}\boldsymbol{\xi}_h^{j+1}(\mathbf{x}) + \frac{t_{j+1}-t}{k}\boldsymbol{\xi}_h^{j}(\mathbf{x}),$$
$$\tilde{\boldsymbol{\xi}}^-(t,\mathbf{x}) := \boldsymbol{\xi}_h^j(\mathbf{x}), \quad \tilde{\boldsymbol{\xi}}^+(t,\mathbf{x}) := \boldsymbol{\xi}_h^{j+1}(\mathbf{x}), \quad \overline{\tilde{\boldsymbol{\xi}}}(t,\mathbf{x}) := \overline{\boldsymbol{\xi}}_h^{j+1/2}.$$

Given any $T' \geq 0$, equation (ii) in Lemma 3.1 may be rewritten as

$$\mathcal{E}_{(\tilde{\mathbf{m}}^+,\tilde{\mathbf{H}}^+,\tilde{\mathbf{E}}^+)}(T') + \frac{\alpha\mu_0}{1+\alpha^2}\int_0^{T'} ||\tilde{\mathbf{m}}_t||_h^2 \,\mathrm{d}t + \sigma\int_0^{T'} \|\overline{\tilde{\mathbf{E}}}\|_{L^2(\omega)}^2 \,\mathrm{d}t \tag{3.1}$$
$$\leq \mathcal{E}_{(\tilde{\mathbf{m}}_0,\tilde{\mathbf{H}}_0,\tilde{\mathbf{E}}_0)}(0) + \int_0^{T'} (\overline{\tilde{\mathbf{J}}},\overline{\tilde{\mathbf{E}}})\,\mathrm{d}t.$$

We define $\mathbf{P}_{\mathbf{Y}_h} : L^2(\Omega,\mathbb{R}^3) \to \mathbf{Y}_h$ through $(\mathbf{u} - \mathbf{P}_{\mathbf{Y}_h}\mathbf{u}, \boldsymbol{\varphi}_h) = 0$ for all $\boldsymbol{\varphi}_h \in \mathbf{Y}_h$ and all $\mathbf{u} \in L^2(\Omega,\mathbb{R}^3)$. Letting $\big(\boldsymbol{\phi}_h, \boldsymbol{\varphi}_h, \boldsymbol{\mathfrak{Z}}_h\big)(t,\cdot) := \big(\boldsymbol{\mathcal{I}}_{\mathbf{V}_h}\boldsymbol{\phi}, \boldsymbol{\mathcal{I}}_{\mathbf{X}_h}\boldsymbol{\varphi}, \mathbf{P}_{\mathbf{Y}_h}\boldsymbol{\mathfrak{Z}}\big)(t,\cdot)$ for $\boldsymbol{\phi} \in C^\infty(\omega_T;\mathbb{R}^3)$ and $\boldsymbol{\mathfrak{Z}}, \boldsymbol{\varphi} \in \mathcal{D}\big([0,T); C^\infty(\Omega,\mathbb{R}^3) \cap \mathbf{H}_0(\mathbf{curl},\Omega)\big)$ we may rewrite Algorithm 1.2 as follows:

$$\int_0^T (\tilde{\mathbf{m}}_t, \boldsymbol{\phi}_h)_h \,\mathrm{d}t + \alpha\int_0^T (\tilde{\mathbf{m}}^- \times \tilde{\mathbf{m}}_t, \boldsymbol{\phi}_h)_h \,\mathrm{d}t = (1+\alpha^2)\int_0^T \big(\overline{\tilde{\mathbf{m}}} \times (\tilde{\Delta}_h\overline{\tilde{\mathbf{m}}} + \mathbf{P}_{\mathbf{V}_h}\overline{\tilde{\mathbf{H}}}), \boldsymbol{\phi}_h\big)_h \,\mathrm{d}t, \tag{3.2}$$

$$\varepsilon_0\int_0^T (\tilde{\mathbf{E}}_t, \boldsymbol{\varphi}_h)\,\mathrm{d}t - \int_0^T (\overline{\tilde{\mathbf{H}}}, \nabla\times\boldsymbol{\varphi}_h)\,\mathrm{d}t + \sigma\int_0^T (\chi_\omega\overline{\tilde{\mathbf{E}}}, \boldsymbol{\varphi}_h)\,\mathrm{d}t = \int_0^T (\overline{\tilde{\mathbf{J}}}, \boldsymbol{\varphi}_h)\,\mathrm{d}t, \tag{3.3}$$

$$\mu_0\int_0^T (\tilde{\mathbf{H}}_t, \boldsymbol{\mathfrak{Z}}_h)\,\mathrm{d}t + \int_0^T (\nabla\times\overline{\tilde{\mathbf{E}}}, \boldsymbol{\mathfrak{Z}}_h)\,\mathrm{d}t = -\mu_0\int_0^T (\tilde{\mathbf{m}}_t, \boldsymbol{\mathfrak{Z}}_h)\,\mathrm{d}t. \tag{3.4}$$

The a priori bounds in Lemma 3.1 provide the existence of a triple

$$(\,\mathbf{m},\mathbf{H},\mathbf{E}\,) \in \big[L^\infty\big(0,T;W^{1,2}(\omega,\mathbb{S}^2)\big) \cap W^{1,2}(\omega_T;\mathbb{R}^3)\big] \times \big[L^\infty\big(0,T;L^2(\Omega;\mathbb{R}^3)\big)\big]^2,$$

which is the weak limit (as $k,h \to 0$) of a subsequence $\big\{(\,\tilde{\mathbf{m}},\tilde{\mathbf{H}},\tilde{\mathbf{E}}\,)\big\}_{k,h}$, such that

$$\tilde{\mathbf{m}}, \tilde{\mathbf{m}}^\pm, \overline{\tilde{\mathbf{m}}} \overset{*}{\rightharpoonup} \mathbf{m} \;\text{ in } L^\infty\big(0,T;W^{1,2}(\omega,\mathbb{R}^3)\big), \quad \tilde{\mathbf{m}} \rightharpoonup \mathbf{m} \;\text{ in } W^{1,2}(\omega_T,\mathbb{R}^3),$$
$$\tilde{\mathbf{m}}, \tilde{\mathbf{m}}^\pm\,\overline{\tilde{\mathbf{m}}} \to \mathbf{m} \;\text{ in } L^2(\omega_T,\mathbb{R}^3),$$
$$(\,\tilde{\mathbf{H}}, \tilde{\mathbf{H}}^\pm, \overline{\tilde{\mathbf{H}}}; \tilde{\mathbf{E}}, \tilde{\mathbf{E}}^\pm, \overline{\tilde{\mathbf{E}}}\,) \overset{*}{\rightharpoonup} (\,\mathbf{H};\mathbf{E}\,) \;\text{ in } \big[L^\infty\big((0,T);L^2(\Omega,\mathbb{R}^3)\big)\big]^2.$$

Since $|\,\tilde{\mathbf{m}}^+(\mathbf{x}_\ell)\,| = 1$ for all $\ell \in L$, and all $t \in (0,T)$ by Lemma 3.1, (i), we deduce with a discrete Poincaré inequality that

$$\big\||\tilde{\mathbf{m}}^+|^2 - 1\big\|_{L^2(K)} \leq Ch\,\big\|\nabla\big[|\tilde{\mathbf{m}}^+|^2 - 1\big]\big\|_{L^2(K)} \leq Ch\,\|(\tilde{\mathbf{m}}^+)^T\nabla\tilde{\mathbf{m}}^+\|_{L^2(K)}^2 \leq Ch\,\|\nabla\tilde{\mathbf{m}}^+\|_{L^2(K)}^2$$

for all $K \in \mathcal{T}_h$ and hence that $|\tilde{\mathbf{m}}^+| \to 1$ almost everywhere in Ω_T. In particular, we deduce that $|\mathbf{m}| = 1$ almost everywhere in Ω_T. Owing to item (ii) of Lemma 3.1 and weak lower semicontinuity of norms we verify that $(\,\mathbf{m},\mathbf{H},\mathbf{E}\,)$ satisfies part (4) of Definition 2.1. If $\mathbf{m}_h^0 \to \mathbf{m}_0$ in $L^2(\omega;\mathbb{R}^3)$ as $h \to 0$ then weak continuity of the trace operator yields that $\mathbf{m}(0,\cdot) = \mathbf{m}_0$ in the sense of traces.

Identification of limits in (3.2) apart from the last term can be done as in [3] and we discuss the term which involves $\mathbf{P}_{\mathbf{V}_h}\overline{\tilde{\mathbf{H}}}$. By definition of $\mathbf{P}_{\mathbf{V}_h}$,

$$\begin{aligned}(\overline{\tilde{\mathbf{m}}} \times \mathbf{P}_{\mathbf{V}_h}\overline{\tilde{\mathbf{H}}}, \boldsymbol{\phi}_h)_h &= -(\overline{\tilde{\mathbf{m}}} \times \boldsymbol{\phi}_h, \mathbf{P}_{\mathbf{V}_h}\overline{\tilde{\mathbf{H}}})_h = -\big(\boldsymbol{\mathcal{I}}_{\mathbf{V}_h}(\overline{\tilde{\mathbf{m}}} \times \boldsymbol{\phi}_h), \mathbf{P}_{\mathbf{V}_h}\overline{\tilde{\mathbf{H}}}\big)_h \\ &= -\big(\boldsymbol{\mathcal{I}}_{\mathbf{V}_h}(\overline{\tilde{\mathbf{m}}} \times \boldsymbol{\phi}_h), \overline{\tilde{\mathbf{H}}}\big) \\ &= -\big((\boldsymbol{\mathcal{I}}_{\mathbf{V}_h} - \mathbf{Id})(\overline{\tilde{\mathbf{m}}} \times \boldsymbol{\phi}_h), \overline{\tilde{\mathbf{H}}}\big) - \big(\overline{\tilde{\mathbf{m}}} \times \boldsymbol{\phi}_h, \overline{\tilde{\mathbf{H}}}\big).\end{aligned}$$

Noting that

$$\big((\boldsymbol{\mathcal{I}}_{\mathbf{V}_h} - \mathbf{Id})(\overline{\tilde{\mathbf{m}}} \times \boldsymbol{\phi}_h), \overline{\tilde{\mathbf{H}}}\big) \leq Ch^2 \sum_{K \in \mathcal{T}_h} \| D^2(\overline{\tilde{\mathbf{m}}} \times \boldsymbol{\phi}_h) \|_{L^2(K)} \| \overline{\tilde{\mathbf{H}}} \|_{L^2(K)}$$
$$\leq Ch^2 \| \nabla \overline{\tilde{\mathbf{m}}} \|_{L^2} \| \nabla \boldsymbol{\phi}_h \|_{L^\infty} \| \overline{\tilde{\mathbf{H}}} \|_{L^2}$$

we deduce that

$$\int_0^T \big(\overline{\tilde{\mathbf{m}}} \times \mathbf{P}_{\mathbf{V}_h} \overline{\tilde{\mathbf{H}}}, \boldsymbol{\phi}_h\big)_h \,\mathrm{d}t \to \int_0^T (\mathbf{m} \times \mathbf{H}, \boldsymbol{\phi})$$

as $h, k \to 0$. To identify the limit in (3.3), we use the identity

$$\int_0^T (\tilde{\mathbf{E}}_t, \boldsymbol{\varphi}_h)\,\mathrm{d}t = -\int_0^T \big(\tilde{\mathbf{E}}, (\boldsymbol{\varphi}_h)_t\big)\,\mathrm{d}t + \big(\mathbf{E}(T,\cdot), \boldsymbol{\varphi}_h(T,\cdot)\big) - \big(\mathbf{E}(0,\cdot), \boldsymbol{\varphi}_h(0,\cdot)\big)\,,$$

and a passage to the limits in the terms on the right-hand side is straightforward owing to their linearity and the convergence properties of $\tilde{\mathbf{E}}$; we proceed accordingly with the leading term in (3.3). It remains to consider the second term in (3.4). Owing to $\nabla \times \mathbf{X}_h \subset \mathbf{Y}_h$, $\mathfrak{z}_h = \mathbf{P}_{\mathbf{Y}_h}\mathfrak{z}$, and the properties of $\overline{\tilde{\mathbf{E}}}$ we verify

$$\int_0^T (\nabla \times \overline{\tilde{\mathbf{E}}}, \mathfrak{z}_h) dt = \int_0^T (\nabla \times \overline{\tilde{\mathbf{E}}}, \mathfrak{z}) dt = \int_0^T (\overline{\tilde{\mathbf{E}}}, \nabla \times \mathfrak{z})\,\mathrm{d}t \to \int_0^T (\mathbf{E}, \nabla \times \mathfrak{z})\,\mathrm{d}t\,.$$

Finally, weak lower semicontinuity of norms and strong convergence of discrete initial data implies the energy inequality in item (4) of Definition 2.1 for the limit $(\mathbf{m}, \mathbf{E}, \mathbf{H})$. We have thus proved the following theorem.

Theorem 3.1. *Let* (2.8)–(2.9) *be valid. Suppose that we have* $|\mathbf{m}_h^0(\mathbf{x}_\ell)| = 1$ *for all* $\ell \in L$ *and let* $\{(\mathbf{m}_h^j, \mathbf{E}_h^j, \mathbf{H}_h^j)\}_{j\geq 0}$ *solve Algorithm 1.2. Assume that* $\mathbf{m}_h^0 \to \mathbf{m}_0$ *in* $W^{1,2}(\omega)$ *and* $(\tilde{\mathbf{H}}_h^0, \tilde{\mathbf{E}}_h^0) \to (\mathbf{H}_0, \mathbf{E}_0)$ *in* $L^2(\Omega, \mathbb{R}^3)$ *as* $h \to 0$ *and let* $T > 0$ *be a fixed constant. As* $k, h \to 0$, *a subsequence of* $(\tilde{\mathbf{m}}, \tilde{\mathbf{H}}, \tilde{\mathbf{E}})$ *converges weakly to* $(\mathbf{m}, \mathbf{H}, \mathbf{E})$ *in* $\big[L^\infty\big(0,T; W^{1,2}(\Omega, \mathbb{S}^2)\big) \cap W^{1,2}(\omega_T, \mathbb{R}^3)\big] \times \big[L^\infty\big((0,T); L^2(\Omega, \mathbb{R}^3)\big)\big]^2$, *and* $(\mathbf{m}, \mathbf{H}, \mathbf{E})$ *is a weak solution of* (1.1)–(1.3).

In fact, every weak accumulation point of $(\tilde{\mathbf{m}}, \tilde{\mathbf{H}}, \tilde{\mathbf{E}})$ solves (1.1)–(1.3). Note also that no discrete version of the compatibility assumption (2.9) is assumed for $(\tilde{\mathbf{H}}_h^0, \tilde{\mathbf{E}}_h^0, \mathbf{m}_h^0)$.

4. Solving the nonlinear system

We employ a fixed-point iteration to solve the nonlinear system in each step of Algorithm 1.2: Given $\mathbf{m}_h^j$, $\mathbf{H}_h^j$, and $\mathbf{E}_h^j$ (or approximations $\tilde{\mathbf{m}}_h^j$, $\tilde{\mathbf{H}}_h^j$, and $\tilde{\mathbf{E}}_h^j$) we aim at approximating $\mathbf{w}_h := \overline{\mathbf{m}}_h^{j+1/2}$, $\mathbf{F}_h := \overline{\mathbf{E}}_h^{j+1/2}$, and $\mathbf{G}_h := \overline{\mathbf{H}}_h^{j+1/2}$. The time derivative $d_t\mathbf{m}_h^{j+1}$ is replaced by $\frac{2}{k}(\mathbf{w}_h - \mathbf{m}_h^j)$ and similar expressions for $d_t\mathbf{E}_h^{j+1}$ and $d_t\mathbf{H}_h^{j+1}$. A linearization of the nonlinear term $\big(\mathbf{w}_h \times (\tilde{\Delta}_h \mathbf{w}_h + \mathbf{P}_{\mathbf{L}^2}\mathbf{G}_h), \boldsymbol{\phi}_h\big)_h$ and the identity $\mathbf{m}_h^j \times d_t\mathbf{m}_h^{j+1} = -\frac{2}{k}\overline{\mathbf{m}}_h^{j+1/2} \times \mathbf{m}_h^j$ lead to the following algorithm.

Algorithm 4.1. *Set* $(\mathbf{w}_h^0, \mathbf{F}_h^0, \mathbf{G}_h^0) := (\tilde{\mathbf{m}}_h^j, \tilde{\mathbf{E}}_h^j, \tilde{\mathbf{H}}_h^j)$ *and* $\ell := 0$.
(i) Compute $(\mathbf{w}_h^{\ell+1}, \mathbf{F}_h^{\ell+1}, \mathbf{G}_h^{\ell+1}) \in \mathbf{V}_h \times \mathbf{X}_h^0 \times \mathbf{Y}_h$ *such that for all* $(\boldsymbol{\phi}_h, \boldsymbol{\varphi}_h, \mathfrak{z}_h) \in \mathbf{V}_h \times \mathbf{X}_h^0 \times \mathbf{Y}_h$

there holds

$$
(4.1)\quad
\begin{aligned}
&\frac{2}{k}(\mathbf{w}_h^{\ell+1},\boldsymbol{\phi}_h)_h-\frac{2\alpha}{k}(\mathbf{w}_h^{\ell+1}\times\tilde{\mathbf{m}}_h^j,\boldsymbol{\phi}_h)_h\\
&\qquad-(1+\alpha^2)\big(\mathbf{w}_h^{\ell+1}\times(\tilde{\Delta}_h\mathbf{w}_h^{\ell}+\mathbf{P}_{\mathbf{V}^h}\mathbf{G}_h^{\ell}),\boldsymbol{\phi}_h\big)_h=\frac{2}{k}(\tilde{\mathbf{m}}_h^j,\boldsymbol{\phi}_h)_h,\\
&\frac{2\varepsilon_0}{k}\,(\mathbf{F}_h^{\ell+1},\boldsymbol{\varphi}_h)-(\mathbf{G}_h^{\ell+1},\nabla\times\boldsymbol{\varphi}_h)+\sigma(\chi_\omega\mathbf{F}_h^{\ell+1},\boldsymbol{\varphi}_h)=\frac{2\varepsilon_0}{k}\,(\tilde{\mathbf{E}}_h^j,\boldsymbol{\varphi}_h)-(\overline{\mathbf{J}}_h^{j+1/2},\boldsymbol{\varphi}_h),\\
&\frac{2\mu_0}{k}\,(\mathbf{G}_h^{\ell+1},\boldsymbol{\mathfrak{z}}_h)+(\nabla\times\mathbf{F}_h^{\ell+1},\boldsymbol{\mathfrak{z}}_h)+\frac{2\mu_0}{k}\,(\mathbf{w}_h^{\ell+1},\boldsymbol{\mathfrak{z}}_h)=\frac{2\mu_0}{k}\,(\tilde{\mathbf{H}}_h^j,\boldsymbol{\mathfrak{z}}_h)+\frac{2\mu_0}{k}\,(\tilde{\mathbf{m}}_h^j,\boldsymbol{\mathfrak{z}}_h).
\end{aligned}
$$

(ii) Stop and set $(\tilde{\mathbf{m}}_h^{j+1},\tilde{\mathbf{E}}_h^{j+1},\tilde{\mathbf{H}}_h^{j+1}):=2(\mathbf{w}_h^{\ell+1},\mathbf{F}_h^{\ell+1},\mathbf{G}_h^{\ell+1})-(\tilde{\mathbf{m}}_h^j,\tilde{\mathbf{E}}_h^j,\tilde{\mathbf{H}}_h^j)$, *once*

$$
(4.2)\quad ||\tilde{\Delta}_h(\mathbf{w}_h^{\ell+1}-\mathbf{w}_h^{\ell})||_h+||\mathbf{G}_h^{\ell+1}-\mathbf{G}_h^{\ell}||_{L^2}\le\varepsilon.
$$

(iii) Set $\ell:=\ell+1$ *and go to (i).*

For $\varepsilon\to 0$, the output of the iteration converges to the solution of (1.7)–(1.9) (in case $\tilde{\mathbf{m}}_h^j=\mathbf{m}_h^j$, $\tilde{\mathbf{E}}_h^j=\mathbf{E}_h^j$, and $\tilde{\mathbf{H}}_h^j=\mathbf{H}_h^j$) provided that $k\le ch_{min}^2/(1+\alpha^2)$ with a factor $c>0$ that only depends on the geometry of $\mathcal{T}_h$.

Lemma 4.1. *Suppose that* $||\tilde{\mathbf{m}}_h^j||_{L^\infty}\le c_0$. *For all* $\ell\ge 0$ *there exists a unique* $(\mathbf{w}_h^{\ell+1},\mathbf{F}_h^{\ell+1},\mathbf{G}_h^{\ell+1})$ *solving* (4.1) *and there holds*

$$
(4.3)\quad
\begin{aligned}
&\sqrt{\mu_0/2}||\mathbf{w}_h^{\ell+1}-\mathbf{w}_h^{\ell}||_h+\sqrt{2\varepsilon_0}||\mathbf{F}_h^{\ell+1}-\mathbf{F}_h^{\ell}||_{L^2}+\sqrt{\mu_0}||\mathbf{G}_h^{\ell+1}-\mathbf{G}_h^{\ell}||_{L^2}\\
&\qquad\qquad\le\Theta\Big(\sqrt{\mu_0/2}||\mathbf{w}_h^{\ell}-\mathbf{w}_h^{\ell-1}||_h+\sqrt{\mu_0}||\mathbf{G}_h^{\ell}-\mathbf{G}_h^{\ell-1}||_{L^2}\Big)
\end{aligned}
$$

with $\Theta=c_1^2c_0\sqrt{15}(1+\alpha^2)kh_{min}^{-2}$ *provided that* $c_1^2\sqrt{5}h_{min}^{-2}\ge 1$. *Let* $(\tilde{\mathbf{m}}_h^{j+1},\tilde{\mathbf{E}}_h^{j+1},\tilde{\mathbf{H}}_h^{j+1})$ *be the output of Algorithm 4.1. There exists a function* $\mathbf{R}^j\in\mathbf{V}_h$ *satisfying* $||\mathbf{R}^j||_h\le\varepsilon$ *such that for all* $(\boldsymbol{\phi}_h,\boldsymbol{\varphi}_h,\boldsymbol{\mathfrak{z}}_h)\in\mathbf{V}_h\times\mathbf{X}_h^0\times\mathbf{Y}_h$ *there holds*

$$
(4.4)\quad
\begin{aligned}
&(d_t\tilde{\mathbf{m}}_h^{j+1},\boldsymbol{\phi}_h)_h+\alpha(\tilde{\mathbf{m}}_h^j\times d_t\tilde{\mathbf{m}}_h^{j+1},\boldsymbol{\phi}_h)_h\\
&\quad-(1+\alpha^2)\big(\overline{\tilde{\mathbf{m}}}_h^{j+1/2}\times(\tilde{\Delta}_h\overline{\tilde{\mathbf{m}}}_h^{j+1/2}+\mathbf{P}_{\mathbf{V}^h}\overline{\tilde{\mathbf{H}}}_h^{j+1/2}),\boldsymbol{\phi}_h\big)_h=(1+\alpha^2)\big(\overline{\tilde{\mathbf{m}}}_h^{j+1/2}\times\mathbf{R}^j,\boldsymbol{\phi}_h\big)_h,\\
&\frac{\varepsilon_0}{k}\,(d_t\tilde{\mathbf{E}}_h^{j+1},\boldsymbol{\varphi}_h)-(\overline{\tilde{\mathbf{E}}}_h^{j+1/2},\nabla\times\boldsymbol{\varphi}_h)+\sigma(\chi_\omega\overline{\tilde{\mathbf{E}}}_h^{j+1/2},\boldsymbol{\varphi}_h)=-(\overline{\mathbf{J}}_h^{j+1/2},\boldsymbol{\varphi}_h),\\
&\frac{\mu_0}{k}\,(d_t\tilde{\mathbf{H}}_h^{j+1},\boldsymbol{\mathfrak{z}}_h)+(\nabla\times\overline{\tilde{\mathbf{E}}}_h^{j+1/2},\boldsymbol{\mathfrak{z}}_h)+\frac{\mu_0}{k}\,(d_t\tilde{\mathbf{m}}_h^{j+1},\boldsymbol{\mathfrak{z}}_h)=0.
\end{aligned}
$$

Moreover, if $|\tilde{\mathbf{m}}_h^j(\mathbf{x}_m)|=1$ *for all* $m\in L$ *then there holds* $|\tilde{\mathbf{m}}_h^{j+1}(\mathbf{x}_m)|=1$ *for all* $m\in L$.

Proof. Step 1. For $(\boldsymbol{\phi}_h,\boldsymbol{\varphi}_h,\boldsymbol{\mathfrak{z}}_h)=(\mathbf{w}_h^{\ell+1},\mathbf{F}_h^{\ell+1},\mathbf{G}_h^{\ell+1})$ the sum of the left-hand sides in (4.1) (after multiplication of the first equation by μ_0) equals

$$
\frac{2\mu_0}{k}||\mathbf{w}_h^{\ell+1}||_h^2+\frac{2\varepsilon_0}{k}||\mathbf{F}_h^{\ell+1}||_{L^2}^2+\sigma||\chi_\omega\mathbf{F}_h^{\ell+1}||_{L^2}^2+\frac{2\mu_0}{k}||\mathbf{G}_h^{\ell+1}||_{L^2}^2+\frac{2\mu_0}{k}(\mathbf{w}_h^{\ell+1},\mathbf{G}_h^{\ell+1}).
$$

Since $2(\mathbf{w}_h^{\ell+1},\mathbf{G}_h^{\ell+1})\ge-||\mathbf{w}_h^{\ell+1}||_h^2-||\mathbf{G}_h^{\ell+1}||_{L^2}^2$ the bilinear form defined by the left-hand side of (4.1) is positive definite on $\big[\mathbf{V}_h\times\mathbf{X}_h^0\times\mathbf{Y}_h\big]^2$ and (4.1) admits a unique solution.
Step 2. We next control $||\mathbf{w}_h^{\ell+1}||_{L^\infty}$ uniformly for all $\ell\ge 0$: Let $m\in L$ be such that $||\mathbf{w}_h^{\ell+1}||_{L^\infty}=|\mathbf{w}_h^{\ell+1}(\mathbf{x}_m)|$. Putting $\boldsymbol{\phi}_h=\varphi_m\mathbf{w}_h^{\ell+1}(\mathbf{x}_m)$ in the first equation of (4.1) leads to

$$
(4.5)\quad ||\mathbf{w}_h^{\ell+1}||_{L^\infty}=|\mathbf{w}_h^{\ell+1}(\mathbf{x}_m)|\le|\tilde{\mathbf{m}}_h^j(\mathbf{x}_m)|\le||\tilde{\mathbf{m}}_h^j||_{L^\infty}\le c_0.
$$

Step 3. Subtraction of two subsequent equations of iteration (4.1) shows

$$\begin{aligned}
&\frac{2}{k}(\mathbf{w}_h^{\ell+1}-\mathbf{w}_h^{\ell},\boldsymbol{\phi}_h)_h-\frac{2\alpha}{k}\big((\mathbf{w}_h^{\ell+1}-\mathbf{w}_h^{\ell})\times\tilde{\mathbf{m}}_h^j,\boldsymbol{\phi}_h\big)_h\\
&\quad-(1+\alpha^2)\big((\mathbf{w}_h^{\ell+1}-\mathbf{w}_h^{\ell})\times(\tilde{\Delta}_h\mathbf{w}_h^{\ell}+\mathbf{P}_{\mathbf{V}^h}\mathbf{G}_h^{\ell}),\boldsymbol{\phi}_h\big)_h\\
&\quad-(1+\alpha^2)\big(\mathbf{w}_h^{\ell}\times[(\tilde{\Delta}_h\mathbf{w}_h^{\ell}+\mathbf{P}_{\mathbf{V}^h}\mathbf{G}_h^{\ell})-(\tilde{\Delta}_h\mathbf{w}_h^{\ell-1}+\mathbf{P}_{\mathbf{V}^h}\mathbf{G}_h^{\ell-1})],\boldsymbol{\phi}_h\big)_h=0,\\
&\frac{2\varepsilon_0}{k}(\mathbf{F}_h^{\ell+1}-\mathbf{F}_h^{\ell},\boldsymbol{\varphi}_h)-(\mathbf{G}_h^{\ell+1}-\mathbf{G}_h^{\ell},\nabla\times\boldsymbol{\varphi}_h)+\sigma\big(\chi_\omega(\mathbf{F}_h^{\ell+1}-\mathbf{F}_h^{\ell}),\boldsymbol{\varphi}_h\big)=0,\\
&\frac{2\mu_0}{k}(\mathbf{G}_h^{\ell+1}-\mathbf{G}_h^{\ell},\boldsymbol{\zeta}_h)+\big(\nabla\times(\mathbf{F}_h^{\ell+1}-\mathbf{F}_h^{\ell}),\boldsymbol{\zeta}_h\big)+\frac{2\mu_0}{k}(\mathbf{w}_h^{\ell+1}-\mathbf{w}_h^{\ell},\boldsymbol{\zeta}_h)=0.
\end{aligned}$$

Adding the three identities (after multiplying the first equation by μ_0) and choosing $(\boldsymbol{\phi}_h,\boldsymbol{\varphi}_h,\boldsymbol{\zeta}_h)=(\mathbf{w}_h^{\ell+1}-\mathbf{w}_h^{\ell},\mathbf{F}_h^{\ell+1}-\mathbf{F}_h^{\ell},\mathbf{G}_h^{\ell+1}-\mathbf{G}_h^{\ell})$ provides

$$\begin{aligned}
&\frac{2\mu_0}{k}\|\mathbf{w}_h^{\ell+1}-\mathbf{w}_h^{\ell}\|_h^2+\frac{2\varepsilon_0}{k}\|\mathbf{F}_h^{\ell+1}-\mathbf{F}_h^{\ell}\|_{L^2}^2+\sigma\|\chi_\omega(\mathbf{F}_h^{\ell+1}-\mathbf{F}_h^{\ell})\|_{L^2}^2+\frac{2\mu_0}{k}\|\mathbf{G}_h^{\ell+1}-\mathbf{G}_h^{\ell}\|_{L^2}^2\\
&\quad=-\frac{2\mu_0}{k}(\mathbf{w}_h^{\ell+1}-\mathbf{w}_h^{\ell},\mathbf{G}_h^{\ell+1}-\mathbf{G}_h^{\ell})\\
&\qquad+\mu_0(1+\alpha^2)\big(\mathbf{w}_h^{\ell}\times[(\tilde{\Delta}_h\mathbf{w}_h^{\ell}+\mathbf{P}_{\mathbf{V}^h}\mathbf{G}_h^{\ell})-(\tilde{\Delta}_h\mathbf{w}_h^{\ell-1}+\mathbf{P}_{\mathbf{V}^h}\mathbf{G}_h^{\ell-1})],\mathbf{w}_h^{\ell+1}-\mathbf{w}_h^{\ell}\big)_h\\
&\quad\leq\frac{3\mu_0}{2k}\|\mathbf{w}_h^{\ell+1}-\mathbf{w}_h^{\ell}\|_h^2+\frac{\mu_0}{k}\|\mathbf{G}_h^{\ell+1}-\mathbf{G}_h^{\ell}\|_{L^2}^2\\
&\qquad+k\frac{\mu_0}{2}(1+\alpha^2)^2c_0^2\big(\|\tilde{\Delta}_h(\mathbf{w}_h^{\ell}-\mathbf{w}_h^{\ell-1})\|_h+\|\mathbf{P}_{\mathbf{V}^h}(\mathbf{G}_h^{\ell}-\mathbf{G}_h^{\ell-1})\|_h\big)^2.
\end{aligned}$$

The estimates $\|\tilde{\Delta}_h\boldsymbol{\phi}_h\|_h\leq c_1^2\sqrt{5}h_{min}^{-2}\|\boldsymbol{\phi}_h\|_h$ and $\|\mathbf{P}_{\mathbf{V}^h}\boldsymbol{\zeta}_h\|_h\leq\|\boldsymbol{\zeta}_h\|_{L^2}$ imply (4.3).
Step 4. In order to prove (4.4) we replace $d_t\tilde{\mathbf{m}}_h^{j+1}=\frac{2}{k}(\mathbf{w}_h^{\ell+1}-\tilde{\mathbf{m}}_h^j)$, $\overline{\tilde{\mathbf{m}}}_h^{j+1/2}=\mathbf{w}_h^{\ell+1}$, etc. in (4.1) to verify with $\mathbf{R}^j:=(\tilde{\Delta}_h\mathbf{w}_h^{\ell}+\mathbf{P}_{\mathbf{V}^h}\mathbf{G}_h^{\ell})-(\tilde{\Delta}_h\mathbf{w}_h^{\ell+1}+\mathbf{P}_{\mathbf{V}^h}\mathbf{G}_h^{\ell+1})$

$$\begin{aligned}
&(d_t\tilde{\mathbf{m}}_h^{j+1},\boldsymbol{\phi}_h)_h-\frac{2\alpha}{k}(\overline{\tilde{\mathbf{m}}}_h^{j+1/2}\times\tilde{\mathbf{m}}_h^j,\boldsymbol{\phi}_h)_h\\
&\quad-(1+\alpha^2)\big(\overline{\tilde{\mathbf{m}}}_h^{j+1/2}\times(\tilde{\Delta}_h\overline{\tilde{\mathbf{m}}}_h^{j+1/2}+\mathbf{P}_{\mathbf{V}^h}\overline{\tilde{\mathbf{H}}}_h^{j+1/2}),\boldsymbol{\phi}_h\big)_h=(1+\alpha^2)\big(\overline{\tilde{\mathbf{m}}}_h^{j+1/2}\times\mathbf{R}^j,\boldsymbol{\phi}_h\big)_h,\\
&\frac{\varepsilon_0}{k}(d_t\tilde{\mathbf{E}}_h^{j+1},\boldsymbol{\varphi}_h)-(\overline{\tilde{\mathbf{E}}}_h^{j+1/2},\nabla\times\boldsymbol{\varphi}_h)+\sigma(\chi_\omega\overline{\tilde{\mathbf{E}}}_h^{j+1/2},\boldsymbol{\varphi}_h)=-(\overline{\mathbf{J}}_h^{j+1/2},\boldsymbol{\varphi}_h),\\
&\frac{\mu_0}{k}(d_t\tilde{\mathbf{H}}_h^{j+1},\boldsymbol{\zeta}_h)+(\nabla\times\overline{\tilde{\mathbf{E}}}_h^{j+1/2},\boldsymbol{\zeta}_h)+\frac{\mu_0}{k}(d_t\tilde{\mathbf{m}}_h^{j+1},\boldsymbol{\zeta}_h)=0.
\end{aligned}$$

Using $\frac{2}{k}\overline{\tilde{\mathbf{m}}}_h^{j+1/2}\times\tilde{\mathbf{m}}_h^j=-\tilde{\mathbf{m}}_h^j\times d_t\tilde{\mathbf{m}}_h^{j+1}$ we verify (4.4) and the stopping criterion implies $\|\mathbf{R}\|_h\leq\varepsilon$.
Step 5. We choose $\boldsymbol{\phi}_h=\varphi_m\overline{\tilde{\mathbf{m}}}_h^{j+1/2}(\mathbf{x}_m)$ in (4.4) to verify $d_t|\tilde{\mathbf{m}}_h^{j+1}(\mathbf{x}_m)|^2=0$. □

Remark 4.1. *Convergence to a weak solution of (MLLG) of approximations satisfying* (4.4) *as* $(k,h,\varepsilon)\to 0$ *such that* $\varepsilon=o(h_{min}^2)$ *is verified as in Section 3. The only difference is a perturbed* *energy law: instead of (ii) in Lemma 3.1 one has*

$$\mathcal{E}_h\big(\{\tilde{\mathbf{m}}_h^{j+1},\tilde{\mathbf{H}}_h^{j+1},\tilde{\mathbf{E}}_h^{j+1}\}\big)+k\sum_{\ell=0}^{j}(1-\varepsilon)\frac{\alpha\mu_0}{1+\alpha^2}\|\,d_t\tilde{\mathbf{m}}_h^{\ell+1}\,\|_h^2+\sigma\,\|\,\overline{\tilde{\mathbf{E}}}_h^{\ell+1/2}\,\|_{L^2(\omega)}^2$$

$$\leq \mathcal{E}_h\big(\{\tilde{\mathbf{m}}_h^{0},\tilde{\mathbf{H}}_h^{0},\tilde{\mathbf{E}}_h^{0}\}\big)-k\sum_{\ell=0}^{j}(\overline{\mathbf{J}}_h^{\ell+1/2},\overline{\tilde{\mathbf{E}}}_h^{\ell+1/2})$$

$$+k\sum_{\ell=0}^{j}\big\{(1+\alpha^2)\|\,\mathbf{R}^\ell\,\|_h\big(c_3h_{min}^{-2}+\|\,\tilde{\mathbf{H}}_h^{\ell+1/2}\,\|\big)+\frac{1}{4\varepsilon}(1+\alpha^2)\alpha\|\,\mathbf{R}^\ell\,\|_h^2\big\}.$$

5. Computational Experiments

5.1. **Physical model.** In below, let $\mathbf{j}=\frac{\mathbf{J}}{M_s}$, $\mathbf{h}=\frac{\mathbf{H}}{M_s}$ and $\mathbf{e}=\frac{\mathbf{E}}{M_s}$ denote the scaled electric current, magnetic and electric fields, respectively.

In practical computations, the following physical constants have to be included in the model: the permeability of vacuum μ_0^*, the permittivity of vacuum ε_0^*, the exchange constant A^*, the anisotropy constant K^*, the saturation magnetization M_s, and the gyromagnetic ratio γ. The direction of the uniaxial anisotropy is characterized by a unit vector $\mathbf{p}\in\mathbb{S}^2$. Without loss of generality, we assume that $\mathbf{p}$ is parallel to one of the coordinate axes. The effective field then becomes

$$\mathbf{h}_{\text{eff}}=A\Delta\mathbf{m}+K\langle\mathbf{m},\mathbf{p}\rangle\mathbf{p}+\mathbf{h}, \tag{5.1}$$

with constants

$$A=\frac{2A^*}{\mu_0^*M_s^2},\quad K=\frac{2K^*}{\mu_0^*M_s^2}.$$

The LLG equation, which after rescaling in time, takes a dimensionless form

$$\mathbf{m}_t+\alpha\,\mathbf{m}\times\mathbf{m}_t=(1+\alpha^2)\,\mathbf{m}\times\mathbf{h}_{\text{eff}}\quad\text{in}\quad\omega_T\,, \tag{5.2}$$

now corresponds to a fully physical situation with time measured in units of $(\gamma M_s)^{-1}$s, cf., e.g. [19].

To have the same time scales for the whole MLLG system, the Maxwell's equations have to be rescaled in time appropriately. After a change of the time variable and an additional scaling by factor M_s^{-1} we obtain

$$\varepsilon_0\,\mathbf{e}_t+\nabla\times\mathbf{h}+\sigma\,\chi_\omega\mathbf{e}=-\mathbf{j}\quad\text{on}\quad\Omega_{T^*}, \tag{5.3}$$

$$\mu_0\,\mathbf{h}_t-\nabla\times\mathbf{e}=-\mu_0\,\mathbf{m}_t\qquad\text{on}\quad\Omega_{T^*}\,, \tag{5.4}$$

where $\varepsilon_0=\gamma M_s\varepsilon_0^*$, $\mu_0=\gamma M_s\mu_0^*$ and $T^*=\gamma M_s\,T$.

A counterpart of Lemma 3.1, for (5.2)-(5.4) reads as follows.

Lemma 5.1. *Suppose that $|\mathbf{m}_h^0(\mathbf{x}_\ell)|=1$ for all $\ell\in L$. Then the sequence $\{(\mathbf{m}_h^j,\mathbf{E}_h^j,\mathbf{H}_h^j)\}_{j\geq0}$ produced by Algorithm 1.2 satisfies for all $j\geq 0$*

(i) $\quad|\,\mathbf{m}_h^{j+1}(\mathbf{x}_\ell)\,|=1\quad\forall\,\ell\in L\,,$

(ii) $$\mathcal{E}_T:=\mathcal{E}_h^*\big(\{\mathbf{m}_h^{j+1},\mathbf{h}_h^{j+1},\mathbf{e}_h^{j+1}\}\big)+k\sum_{\ell=0}^{j}\frac{\alpha\mu_0M_s}{1+\alpha^2}\|\,d_t\mathbf{m}_h^{\ell+1}\,\|_h^2+\sigma\,\|\,\overline{\mathbf{e}}_h^{\ell+1/2}\,\|_{L^2(\omega)}^2$$

$$=\mathcal{E}_h^*\big(\{\mathbf{m}_h^{0},\mathbf{h}_h^{0},\mathbf{e}_h^{0}\}\big)-k\sum_{\ell=0}^{j}(\overline{\mathbf{j}}_h^{\ell+1/2},\overline{\mathbf{e}}_h^{\ell+1/2})\,,$$

where

$$\begin{aligned}\mathcal{E}_h^*(\{\mathbf{m}_h^j,\mathbf{h}_h^j,\mathbf{e}_h^j\}) &= \frac{\mu_0 M_s}{2}\int_\omega \Big[A|\nabla \mathbf{m}_h^j|^2 + K\boldsymbol{\mathcal{I}}_{\mathbf{V_h}}\Big(1-\langle \mathbf{m}_h^j,\mathbf{p}\rangle^2\Big)\Big]\,\mathrm{d}\mathbf{x}\\ &\quad+\int_\Omega\Big[\frac{\mu_0}{2}\,|\,\mathbf{h}_h^j\,|^2+\frac{\varepsilon_0}{2}\,|\,\mathbf{e}_h^j\,|^2\Big]\,\mathrm{d}\mathbf{x}\\ &:= \mathcal{E}_{ex}+\mathcal{E}_{anis}+\mathcal{E}_H+\mathcal{E}_E\,.\end{aligned}$$

In the following we refer to $\mathcal{E}_T$ as the total energy and to the terms $\mathcal{E}_{ex}$, $\mathcal{E}_{an}$, $\mathcal{E}_H$, $\mathcal{E}_E$ as the exchange energy, anisotropy energy, magnetic field energy, and electric field energy, respectively.

Remark 5.1. *To obtain physically relevant results, the initial condition for the Maxwell-LLG system should satisfy the "divergence-free" constraint from, i.e.,* $\mathrm{div}_h(\mathbf{h}_h^0+\chi_\omega\mathbf{m}_h^0)=0$. *This can be achieved by taking* $\mathbf{h}_h^0=\mathbf{h}_*^0-\chi_\omega(\mathbf{P}_h^*\mathbf{m}_h^0)$*, with* $\mathbf{h}_*^0\in\mathbf{Y}_h$*, s.t.* $\mathrm{div}_h\mathbf{h}_*^0=0$. *The projection* $\mathbf{P}_h^*:\mathbf{V}_h\to\mathbf{Y}_h$ *is for* $\mathbf{u}_h\in\mathbf{V}_h$ *defined through* $(\mathbf{P}_h^*\mathbf{u}_h,\boldsymbol{\mathfrak{z}}_h)=(\mathbf{u}_h,\boldsymbol{\mathfrak{z}}_h)$ *for all* $\boldsymbol{\mathfrak{z}}_h\in\mathbf{Y}_h$*. Since* $\mathbf{m}_h^j$ *is piecewise linear, we have that the value of* $\mathbf{P}_h^*\mathbf{m}_h^j$ *on an element* $K\in\mathcal{T}_h\big|_\omega$ *corresponds to the value of* $\mathbf{m}_h^j$ *in the barycenter of* K*. Further, we have from (1.9) that*

$$\frac{\mu_0}{k}(\mathbf{h}_h^{j+1},\boldsymbol{\mathfrak{z}}_h)+\frac{\mu_0}{k}(\mathbf{P}_h^*\mathbf{m}_h^{j+1},\boldsymbol{\mathfrak{z}}_h)=-(\nabla\times\mathbf{e}_h^{j+1/2},\boldsymbol{\mathfrak{z}}_h)+\frac{\mu_0}{k}(\mathbf{h}_h^j,\boldsymbol{\mathfrak{z}}_h)+\frac{\mu_0}{k}(\mathbf{P}_h^*\mathbf{m}_h^j,\boldsymbol{\mathfrak{z}}_h)\quad\forall\boldsymbol{\mathfrak{z}}_h\in\mathbf{Y}_h.$$

From the previous equation, it can be deduced by induction, that $\mathrm{div}_h(\mathbf{h}_h^{j+1}+\chi_\omega(\mathbf{P}_{\mathbf{Y}_h}\mathbf{m}_h^{j+1}))=0$ *is satisfied pointwise in* Ω*. The above arguments remain valid for (4.1). In our experiments, we simply take* $\mathbf{h}_*^0$ *to be a constant vector field.*

5.2. **Solution of the discrete system.** Without loss of generality, we consider the discrete system with $\sigma=0$. The first equation from (4.1), corresponding to the discrete LLG equation, is efficiently solved by the biconjugate gradient stabilized (BiCGStab) method. The solution of the second and third equations from (4.1) is equivalent to solving a discrete algebraic system of the form

$$\begin{pmatrix}\mathbf{A} & -\mathbf{C}^T\\ \mathbf{C} & \mathbf{B}\end{pmatrix}\begin{pmatrix}\overline{\mathbf{e}}\\ \overline{\mathbf{h}}\end{pmatrix}=\begin{pmatrix}\overline{\mathbf{f}}\\ \overline{\mathbf{g}}\end{pmatrix},\tag{5.5}$$

where

$$\mathbf{A}_{ij}=\frac{2\varepsilon_0}{k}(\boldsymbol{\varphi}_h^i,\boldsymbol{\varphi}_h^j),\quad \mathbf{B}_{ij}=\frac{2\mu_0}{k}(\boldsymbol{\mathfrak{z}}_h^i,\boldsymbol{\mathfrak{z}}_h^j),\quad \mathbf{C}_{ij}=(\nabla\times\boldsymbol{\varphi}_h^j,\boldsymbol{\mathfrak{z}}_h^i),$$

and the vectors of unknowns $\overline{\mathbf{e}}=\{e_i\}$, $\overline{\mathbf{h}}=\{h_i\}$ are defined through

$$\mathbf{F}_h=\sum_i e_i\boldsymbol{\varphi}_h^i,\quad \mathbf{G}_h=\sum_i h_i\boldsymbol{\mathfrak{z}}_h^i.$$

Similarly, we define $\overline{\mathbf{f}}=\{f_i\}$, $\overline{\mathbf{g}}=\{g_i\}$, where $\mathbf{f}=\sum_i f_i\boldsymbol{\varphi}_h^i$ and $\mathbf{g}=\sum_i g_i\boldsymbol{\mathfrak{z}}_h^i$ represent the right-hand sides of the discrete problem.

The system (5.5) can be effectively solved by a preconditioned inexact Uzawa method which consists of two steps:

(1) $\overline{\mathbf{h}}^n=\mathbf{B}^{-1}(\overline{\mathbf{g}}-\mathbf{C}\overline{\mathbf{e}}^n)$,
(2) $\overline{\mathbf{e}}^{n+1}=\overline{\mathbf{e}}^n+\rho\mathbf{S}^{-1}(\overline{\mathbf{f}}+\mathbf{C}^T\overline{\mathbf{h}}^n-\mathbf{A}\overline{\mathbf{e}}^n)$.

Here, $\rho>0$ is a constant (we set $\rho=1$ below), and $\mathbf{S}^{-1}$ is a suitably chosen preconditioner, that can considerably speed up the convergence of the Uzawa iterations. Note that the computation of $\mathbf{B}^{-1}$ in the first step of the above Uzawa algorithm is trivial, since the matrix $\mathbf{B}$ is diagonal, owing to the choice of piecewise constant functions.

The preconditioner $\mathbf{S}$ is an approximation of the Schur complement, i.e.,

$$\mathbf{S}\approx(\mathbf{C}^T\mathbf{B}^{-1}\mathbf{C})+\mathbf{A}.$$

The construction of the preconditioner is motivated by the fact that our formulation can be (formally) considered as a mixed approximation of an eddy current problem of the form

$$\frac{2\varepsilon_0}{k}(\mathbf{F}_h^*, \boldsymbol{\varphi}) + \frac{k}{2\mu_0}(\nabla \times \mathbf{F}_h^*, \nabla \times \boldsymbol{\varphi}) = (\mathbf{f}, \boldsymbol{\varphi}) + \frac{k}{2\mu_0}(\nabla \times \mathbf{g}, \boldsymbol{\varphi}) \qquad \forall \boldsymbol{\varphi} \in \mathbf{H}_0(\mathbf{curl}; \Omega).$$

In matrix notation we have $\mathbf{S} = \mathbf{M} + \mathbf{R}$, with matrices

$$\mathbf{M}_{ij} = \frac{2\varepsilon_0}{k}(\boldsymbol{\varphi}_h^i, \boldsymbol{\varphi}_h^j)\,, \quad \mathbf{R}_{ij} = \frac{k}{2\mu_0}(\nabla \times \boldsymbol{\varphi}_h^i, \nabla \times \boldsymbol{\varphi}_h^j)\,.$$

We compute the approximation of $\mathbf{S}^{-1}$ by the BiCGstab algorithm with at most 50 iterations for every sub-step. A better approximation of $\mathbf{S}^{-1}$ can be obtained by using a multigrid method for eddy current equations, see e.g. [8], which together with the moderate number of outer Uzawa iterations gives an effective method with multigrid complexity.

It is possible to eliminate $\overline{\mathbf{h}}$ from (5.5), which leads to a system of equations in the Schur complement form

$$\left(\mathbf{C}^T\mathbf{B}^{-1}\mathbf{C} + \mathbf{A}\right)\overline{\mathbf{e}} = \overline{\mathbf{f}} + \mathbf{C}^T\mathbf{B}^{-1}\overline{\mathbf{g}}\,. \tag{5.6}$$

An alternative approach to the Uzawa algorithm is to solve equation (5.6) by the conjugate gradient method, see e.g. [17] and the references therein. The conjugate gradient algorithm needs to evaluate $\mathbf{B}^{-1}$, which is trivial, since $\mathbf{B}$ is diagonal. We can speed up the convergence of the conjugate gradient algorithm by using a suitable preconditioner. In our case, one could use the same preconditioner as for the Uzawa algorithm. We use the conjugate gradient algorithm for (5.6) without preconditioning in our experiments, since it proves to be slightly faster than the preconditioned Uzawa algorithm. We expect both methods to have comparable performance with effective multigrid preconditioners, cf. [17].

Remark 5.2. *We observe slow convergence of the algebraic solvers for domains of size $\mathcal{O}(10^{-6})$, i.e., in practical applications. The convergence properties of the solvers improve for larger values of the gyromagnetic ratio γ or for smaller size of the time step k. We believe that the convergence rates can be substantially improved with a suitable multigrid preconditioner. Note that similar problems with solver convergence in micromagnetic applications are reported in* [21]*, where a conjugate gradient algorithm is applied to the eddy current formulation of Maxwell's equations.*

5.3. **Computational results.** Our computational code is based on the finite element package ALBERT, see [22], with tetrahedral meshes in 3D. We use standard piecewise linear elements for the discretization of $\mathbf{m}_h$, with degrees of freedom (DOFs) located at the vortices of the mesh, and piecewise constant elements for $\mathbf{h}_h$ with DOFs located at the barycenters of the mesh elements. We discretize $\mathbf{e}_h$ by edge elements of the first kind, with one DOF per every edge of the mesh. The edge elements of the first kind have only slightly worse approximation properties than the edge element of the second kind, however the latter need two DOFs per edge. In our code we replace (4.2) in Algorithm 4.1 by a slightly more practical stopping criterion for the fixed-point iterations, i.e.,

$$\begin{aligned} ||\mathbf{w}_h^{\ell+1} - \mathbf{w}_h^{\ell}||_h &\leq h^2\varepsilon, \\ ||\mathbf{G}_h^{\ell+1} - \mathbf{G}_h^{\ell}||_{L^2} &\leq \varepsilon. \end{aligned}$$

We choose $\varepsilon = 10^{-8}$ in our computations. The convergence of the fixed-point iterations is attained after at most 6 steps in all presented experiments. We observe monotone decrease of the discrete energy from Lemma 5.1 in all experiments, which confirms good numerical convergence of Algorithm 4.1.

The first example is academic which studies possible finite-time blow-up behavior of weak solutions to (1.1)–(1.5) with the help of Algorithm 1.2. We say that (discrete) finite-time blow-up occurs if the sequence $\left\{||\nabla \mathbf{m}_h^j||_{L^\infty}\right\}_j$ attains the maximum value of the mapping $\mathbf{v}_h \mapsto ||\nabla \mathbf{v}_h||_{L^\infty}$

among functions $\mathbf{v}_h \in \mathbf{V}_h$ satisfying $|\mathbf{v}_h(\mathbf{x}_\ell)| = 1$ for all $\ell \in L$. Corresponding studies are reported in [3, 4] for $\mathbf{h}_{\text{eff}} = \Delta\mathbf{m}$ and $\omega \subset \mathbb{R}^2$, where blow-up is computationally evidenced for supercritical (initial) data. Here, we study the influence of the electromagnetic field $(\mathbf{e}^0, \mathbf{h}^0) : \Omega \to \mathbb{R}^3$ on the supercritical $\mathbf{m}^0 : \omega \to \mathbb{S}^2$.

Example 5.1. *Let* $(0,1)^3 = \omega = \Omega$ *and* $\mathbf{j} \equiv 0$. *Let* $\mathbf{m}^0 : \omega \to \mathbb{S}^2$ *and* $(\mathbf{e}^0, \mathbf{h}^0) : \Omega \to \left[\mathbb{R}^3\right]^2$ *be defined by*

$$\mathbf{m}^0(\mathbf{x}) = \begin{cases} (0,0,-1) & \textit{for } |\mathbf{x}^*| \geq 1/2, \\ (2\mathbf{x}^* A, A^2 - |\mathbf{x}^*|^2)/(A^2 + |\mathbf{x}^*|^2) & \textit{for } |\mathbf{x}^*| \leq 1/2 \textit{ and } \mathbf{x}^* \in \omega \end{cases}$$
$$\mathbf{h}^0_*(\mathbf{x}) = (0,0,H_s) \qquad \textit{in } \Omega\,,$$
$$\mathbf{e}^0(\mathbf{x}) = (0,0,0) \qquad \textit{in } \Omega$$

with $\mathbf{x}^* = (x_1 - 0.5, x_2 - 0.5, 0)$ *and* $A = (1-2|\mathbf{x}^*|)^4/4$. *The computational domain* $\Omega = \omega = (0,1)^3$ *is partitioned into uniform cubes with side h, each cube consists of six tetrahedra. We choose the time step* $k = 10^{-5}$ *and set the other parameters* $\alpha = \gamma = M_s = \mu_0 = 1$, $\varepsilon_0 = 10^{-6}$, $K = 0$.

The constant H_s represents the strength of initial field in the x_3-direction. We computed the experiments for $H_s = -30, 0, 30$ on meshes with $h = 1/2^4$ and $h = 1/2^5$. The evolution of $\|\nabla \mathbf{m}_h\|_\infty$ is depicted in Figure 1. The evolution of the exchange energy can be found in Figure 2. Figure 3 displays the evolution of $\|\mathbf{h}_h\|_\infty / H_s$. We deduce from the Figures 1 and 3 that variations of $\|\nabla \mathbf{m}_h\|_\infty$ close to a certain time $T^* > 0$ ('blow-up time') correspond to variations of $\|\mathbf{h}_h\|_\infty$ close to the same time T^*. A similar behavior is found for the evolution of $\|\mathbf{e}_h\|_\infty$ which is depicted in Figure 4. Further, we observe that the mesh size not only determines the quantity $\max_t \|\nabla \mathbf{m}_h(t,\cdot)\|_\infty$, cf. [3, 4], but influences the evolution of $\|\mathbf{h}_h\|_\infty$, $\|\mathbf{e}_h\|_\infty$. The computations with $H_s = -30$ show that negative initial magnetic field accelerates the blow-up of the solution. The evolution becomes more complex for $H_s = 30$; the blow-up time is slightly delayed. Beyond the instability, when the magnetization is aligned along the $(0,0,-1)$ direction, the influence of the magnetic field on the evolution prevails and the magnetization starts to rotate in the opposite direction, i.e. $(0,0,1)$, see Figure 5 for $h = 2^{-4}$. We did not compute beyond the time $t = 0.214$ however it is reasonable to expect that the magnetization will be aligned in the $(0,0,1)$ direction after the steady state is reached. The detail of the solution for $H_s = 30$, $h = 2^{-4}$ near $\mathbf{x} = (0.5, 0.5, 0.5)$ is depicted in Figure 6. There was only little variation of the magnetization in the x_3 direction, we therefore present all results on the cross-cut through the domain at $x_3 = 0.5$.

The following example is derived from a benchmark problem [16, Problem # 1] of a thin uniaxial ferromagnetic film, for which long-time dynamics is studied in [14], in the case $d = 2$. Here, we study the dynamics of the problem for $d = 3$. According to our knowledge, there are no comparable studies for $d = 3$ in the existing literature.

Example 5.2. *Let* $\omega = (0,2) \times (0,1) \times (0,0.02)$, *and* $\Omega = (-0.2, 2.2) \times (-0.2, 1.2) \times (-0.04, 0.06)$ *(the domain dimensions are in* μm*), with*

$$\alpha = 0.5, \quad \gamma = 2.2 \times 10^9, \quad M_s = 8 \times 10^5, \quad K^* = 5 \times 10^2, \quad A^* = 1.3 \times 10^{-11},$$
$$\mathbf{p} = (1,0,0), \quad \varepsilon_0^* = 0.88422 \times 10^{-11}, \quad \mu_0^* = 1.25667 \times 10^{-6}, \quad \sigma = 0$$

and ($\mathbf{j} \equiv \mathbf{0}$)

$$(\mathbf{e}^0, \mathbf{h}^0) = (\mathbf{0}, \mathbf{0}) \quad \textit{in } \Omega\,.$$

The initial condition $\mathbf{m}_h^0$ *is defined by assigning unit vectors with random orientation to every vortex of the mesh.*

The domains Ω and ω are partitioned into bricks of dimension $0.04 \times 0.04 \times 0.02$. Subsequently, the corresponding computational meshes are obtained by subdivision of each brick into six tetrahedra. This partition results in 7956 degrees of freedom for $\mathbf{m}_h$ on ω and 189000, 81325 degrees of freedom for $\mathbf{e}_h$, $\mathbf{h}_h$ on Ω, respectively. We compute on a time interval $(0, 8000)$, using a uniform time step $k = 0.1$.

The evolution of the discrete energies $\mathcal{E}_T$, $\mathcal{E}_{ex}$, $\mathcal{E}_{an}$, $\mathcal{E}_H$, $\mathcal{E}_E$ (i.e., the total, exchange, anisotropy, magnetic field and electric field energy) from Lemma 5.1 is depicted in Figure 7. Snapshots of the magnetization at different time levels can be found in Figure 8; the vectors are colored according to the value of the x_2-component of the magnetization vector. For comparison, Figure 9 shows the evolution of magnetization with the same initial condition computed without taking the coupling with Maxwell's equations into account. The evolution of the discrete energies $\mathcal{E}_T$, $\mathcal{E}_{ex}$, $\mathcal{E}_{an}$ is displayed in Figure 10 (note that, $\mathcal{E}_H = \mathcal{E}_E \equiv 0$). The figures show a clear difference between the two cases.

The data for the last example are taken from [16, Problem # 4]. Here we study the evolution of the magnetization towards a steady state, the so called S-state, cf. [16, Problem # 4].

Example 5.3. *Let* $\omega = (0, 0.5) \times (0, 0.125) \times (0, 0.003)$*, and* $\Omega = (-0.75, 1.25) \times (-0.9375, 1.0625) \times (-0.7665, 0.7695)$ *(in* μm*), with*

$$\alpha = 1., \quad \gamma = 2.2 \times 10^9, \quad M_s = 8 \times 10^5, \quad K^* = 0, \quad A^* = 1.3 \times 10^{-11},$$
$$\varepsilon_0^* = 0.88422 \times 10^{-11}, \quad \mu_0^* = 1.25667 \times 10^{-6}, \quad \sigma = 0$$

and ($\mathbf{j} \equiv \mathbf{0}$)

$$\begin{aligned} \mathbf{m}^0 &= (1, 0, 0) \quad \text{in } \omega\,, \\ \mathbf{h}_*^0 &= (0.01, 0.01, 0.01), \quad \mathbf{e}^0 = \mathbf{0} \quad \text{in } \Omega\,. \end{aligned}$$

The domain ω *is partitioned uniformly into cubes of dimensions* $0.00390625 \times 0.00390625 \times 0.003$*, where each cube consists of six tetrahedra. The non-uniform mesh for the domain* Ω *is constructed in such a way that it is identical to the mesh for* ω *in the region* $\Omega \cap \omega$ *and the mesh size gradually increases away from the overlapping region. A cross-cut through the mesh at* $x_3 = 0$ *is displayed in Figure 11.*

The above discretization of the computational domains results in 25,542 DOFs for $\mathbf{m}_h$ on ω and 138,302, 353,568 DOFs for $\mathbf{e}_h$, $\mathbf{h}_h$, respectively. We employ a uniform time stepping, with $k = 0.01$.

The magnetization at time $T = 300$ is displayed in Figure 12, the vectors are colored according to the x_2-component of the magnetization. Convergence towards the S-state (cf. [16, Problem # 4]) can be observed from the results. No steady state has yet been reached at the final time, however the convergence towards the steady state after the time $T = 300$ has been very slow. The evolution of the discrete energies from Lemma 5.1 is depicted in Figure 13.

6. Concluding Remarks

We devised an implicit discretization of the Maxwell-Landau-Lifshitz-Gilbert system which is based on linear finite elements. For pairs of time-step sizes and mesh-sizes tending simultaneously but independently to zero, we showed that every accumulation point of the sequence of numerical approximations is a weak solution of the continuous equations satisfying an energy inequality. An iterative solver for the solution of the nonlinear system of equations in each time step is proposed and its convergence is proved under the time-step restriction $k \le Ch^2$. The convergence of the nonlinear solver is robust for small values of the damping parameters α. Owing to expected non-uniqueness and possible occurrence of singularities, strong convergence of the (whole) sequence or error estimates cannot be expected unless additional assumptions on an exact solution are made. The use of higher order finite elements for the discretization of $\mathbf{m}$ are beyond the scope of this paper and remain to be analyzed in future work. Our numerical experiments confirm the theoretical results and indicate that finite-time blow-up for MLLG is possible and hence that singular solutions can develop from smooth initial data. Two examples based on standard micromagnetic benchmark problems are computed to demonstrate the potential of the method for practical applications. Further, we constructed a Schur complement preconditioner for a saddle point system of algebraic equations which arise in every iteration of the nonlinear solver. We observed, that the preconditioning dramatically reduced the number of iterations needed for the convergence of the linear solver on structured and unstructured meshes. A multigrid type preconditioner, which is robust with respect to the time step size, is subject to our current research.

References

[1] F. Alouges, A. Soyeur, *On global weak solutions for Landau-Lifshitz equations: existence and nonuniqueness*, Nonl. Analysis, Theory, Meth. & Appl. **18**, pp. 1071–1084 (1992).

[2] F. Alouges, P. Jaisson *Convergence of a finite elements discretization for the Landau Lifshitz equations*, Math. Models Methods Appl. Sci. **16**, pp. 299–316 (2006).

[3] S. Bartels, A. Prohl *Convergence of an implicit finite element method for the Landau-Lifshitz-Gilbert Equation*, SIAM J. Numer. Anal. **44**, pp. 175–199 (2006).

[4] S. Bartels, J. Ko, A. Prohl, *Numerical approximation of Landau-Lifshitz equations and finite time blow up of weak solutions*, Math. Comp. (accepted) (2007).

[5] W. Brown, *Micromagnetics*, Tracts of Physics, Wiley Interscience (1963).

[6] G. Carbou, P. Fabrie, *Time average in micromagnetism*, J. Diff. Eqn.s **147**, pp. 383–409 (1998).

[7] I. Cimrák, *Error estimates for a semi-implicit numerical scheme solving the Landau-Lifshitz equatoin with an exchange field*, IMA J. Numer. Anal. **25**, pp. 611–634 (2005).

[8] R. Hiptmair *Multigrid method for Maxwell's equations* SIAM J. Numer. Anal. **36**, pp. 204–225 (1998).

[9] M. Kružík, A. Prohl, *Recent Developments in Modeling, Analysis and Numerics of Ferromagnetism*, SIAM Review **48**, pp. 439–483 (2006).

[10] L.D. Landau, E.M. Lifshitz, *On the theory of the dispersion of magnetic permeability in ferromagnetic bodies*, Phys. Z. Sowjetunion **8**, pp. 153–169 (1935).

[11] B. Lax, K. Button, *Microwave Ferrites and Ferrimagnetics*, McGraw-Hill (1962).

[12] P.B. Monk, *Finite element methods for Maxwell's equations*, Oxford University Press (2003).

[13] P.B. Monk, O. Vacus, *Error estimates for a numerical scheme for ferromagnetic problems*, SIAM J. Numer. Anal. **36**, pp. 696–716 (1999).

[14] P.B. Monk, O. Vacus, *Accurate discretization of a non-linear micromagnetic problem*, Comput. Meth. Appl. Mech. Engrg. **190**, pp. 5243–5269 (2001).

[15] J. Nédélec, *A new family of mixed finite elements in* $\mathbb{R}^3$, Numer. Math. **50**, pp. 57–81 (1986).

[16] webpage address: `http://www.ctcms.nist.gov/~rdm/mumag.org.html`.

[17] J. Peters, V. Reichelt, A. Reusken *Fast iterative solvers for discrete Stokes equations* SIAM J. Sci. Comput. **27**, pp. 646–666 (2005) .

[18] A. Prohl, *Computational micromagnetism*, Teubner (2001).

[19] C. Serpico, I.D. Mayergoyz, G. Bertotti, *Numerical technique for integration of the Landau-Lifshitz equation*, J. Appl. Phys. **89**, pp. 6991–6993 (2001).

[20] M. Slodička, Ľ. Baňas, *A numerical scheme for a Maxwell-Landau-Lifshitz-Gilbert system*, Appl. Math. Comp. **158**, pp. 79–99 (2004).

[21] J. Sun, F. Collino, P.B. Monk, L. Wang, *An eddy-current and micromagnetism model with applications to disk write heads*, Int. J. Numer. Meth. Engng. **60**, pp. 1673–1698 (2004).

[22] A. Schmidt and K.G. Siebert, *ALBERT—software for scientific computations and applications*, Acta Math. Univ. Comenian. (N.S.) **70**, pp. 105–122 (2000).

[23] A. Visintin, *On Landau-Lifshitz' Equations for ferromagnetism*, Japan J. Appl. Math. **2**, pp. 69–84 (1985).

Department of Mathematics, Heriot-Watt University, Edinburgh, EH14 4AS, United Kingdom
E-mail address: `L.Banas@hw.ac.uk`

Institut für Numerische Simulation, Rheinische Friedrich-Wilhelms-Universität Bonn, Wegelerstrasse 6, D-53115 Bonn, Germany.
E-mail address: `bartels@ins.uni-bonn.de`

Mathematisches Institut, Universität Tübingen, Auf der Morgenstelle 10, D-72076 Tübingen, Germany.
E-mail address: `prohl@na.uni-tuebingen.de`

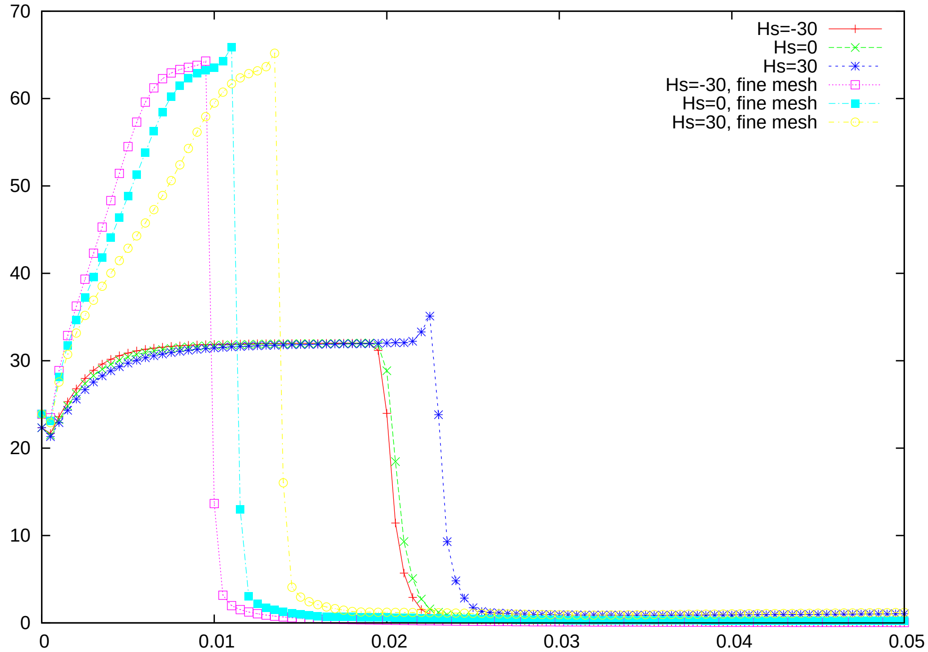

FIGURE 1. Example 5.1: Plot of $t \mapsto \|\nabla \mathbf{m}_h(t, \cdot)\|_\infty$

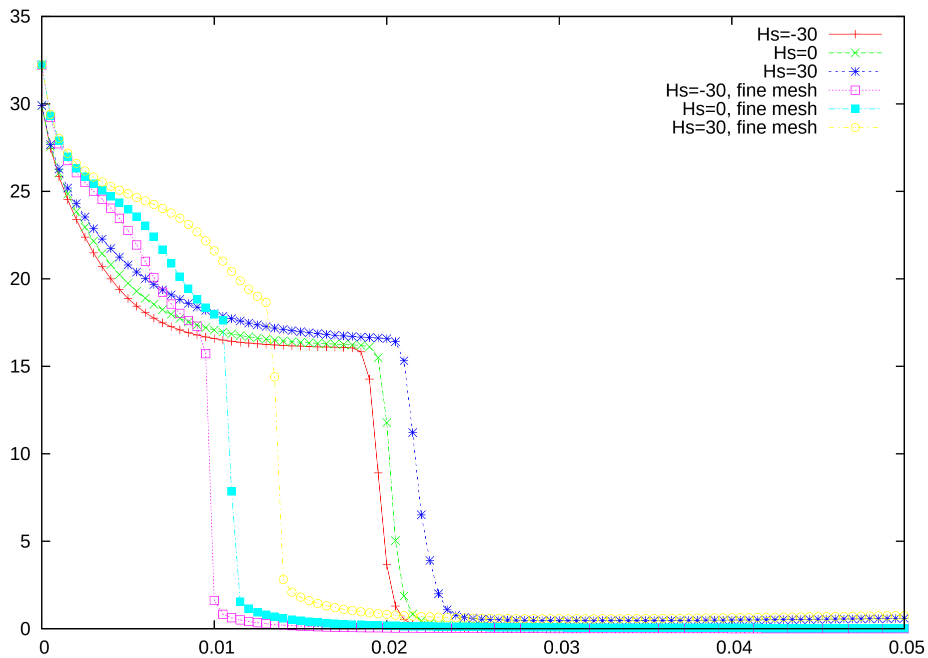

FIGURE 2. Example 5.1: Plot of $t \mapsto \|\nabla \mathbf{m}_h(t, \cdot)\|_2$

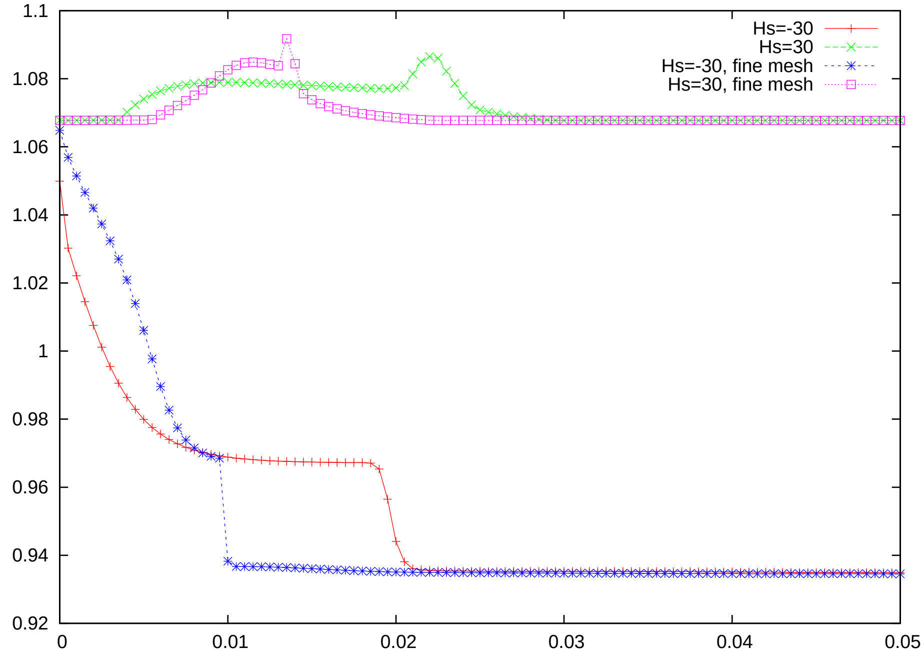

FIGURE 3. Example 5.1: Plot of $t \mapsto \|\mathbf{h}_h(t,\cdot)\|_\infty / |H_s|$

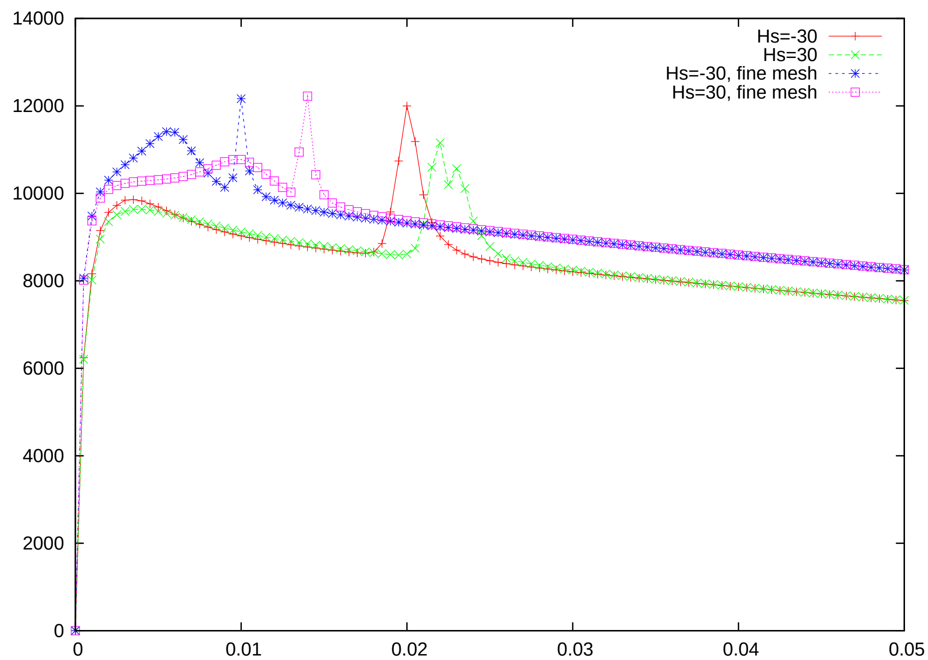

FIGURE 4. Example 5.1: Plot of $t \mapsto \|\mathbf{e}_h(t,\cdot)\|_\infty$

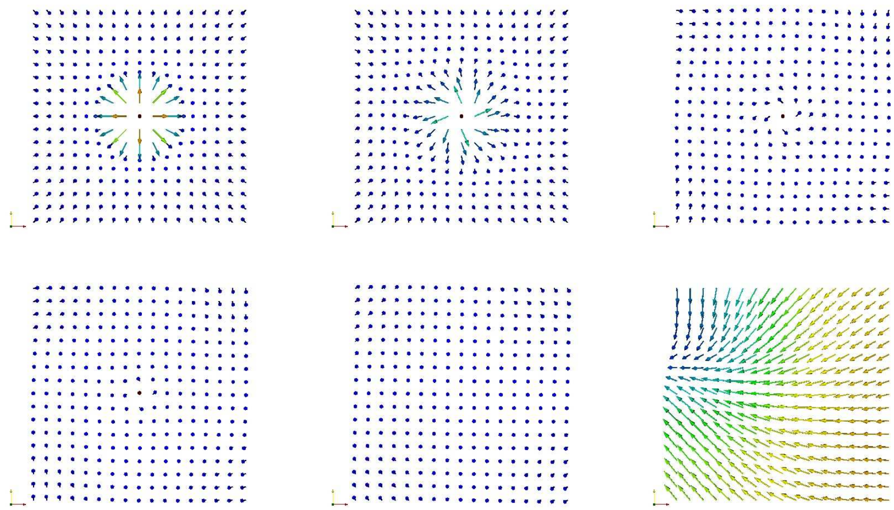

FIGURE 5. Example 5.1: Magnetization for $H_s = 30$ at times $t = 0, 0.01, 0.015, 0.020, 0.030, 0.214$ for $h = 1/2^4$ (from left to right, from top to bottom).

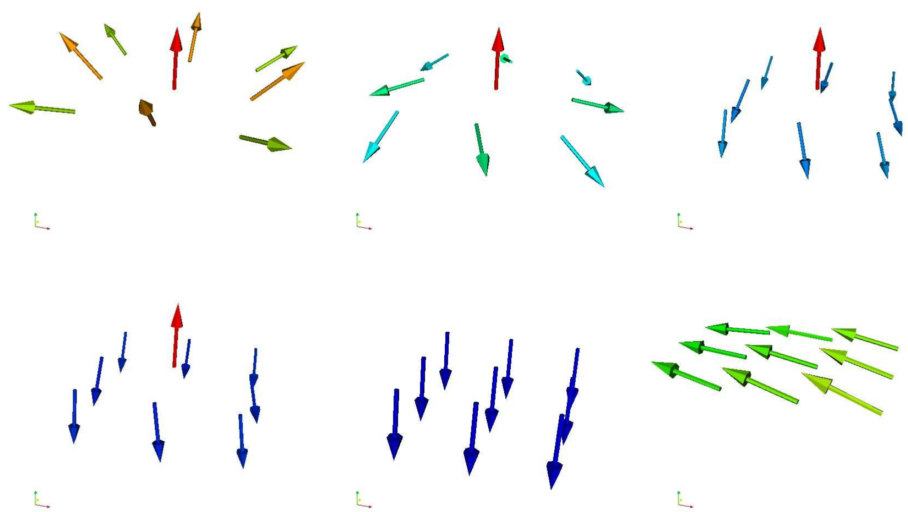

FIGURE 6. Example 5.1: Details of the magnetization for $H_s = 30$ near $\mathbf{x} = (0.5, 0.5, 0.5)$ at times $t = 0, 0.01, 0.015, 0.020, 0.030, 0.214$ for $h = 1/2^4$ (from left to right, from top to bottom).

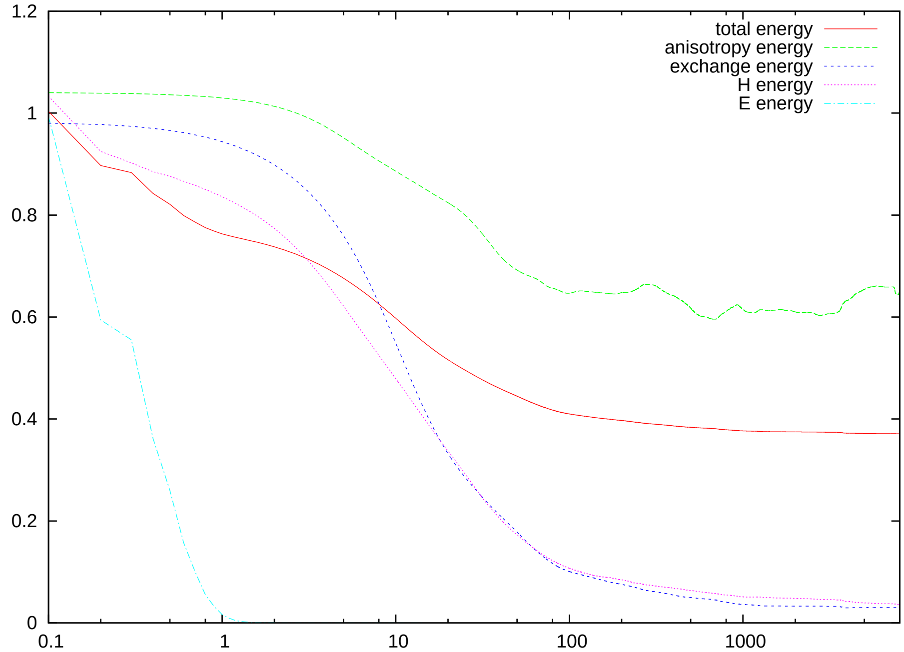

FIGURE 7. Example 5.2: Evolution of the energies, $\log(t) \mapsto \mathcal{E}_T(t)/22$, $\mathcal{E}_{ex}(t)/11$, $\mathcal{E}_{an}(t)/0.04$, $\mathcal{E}_H(t)/7$, $\mathcal{E}_E(t)/4$.

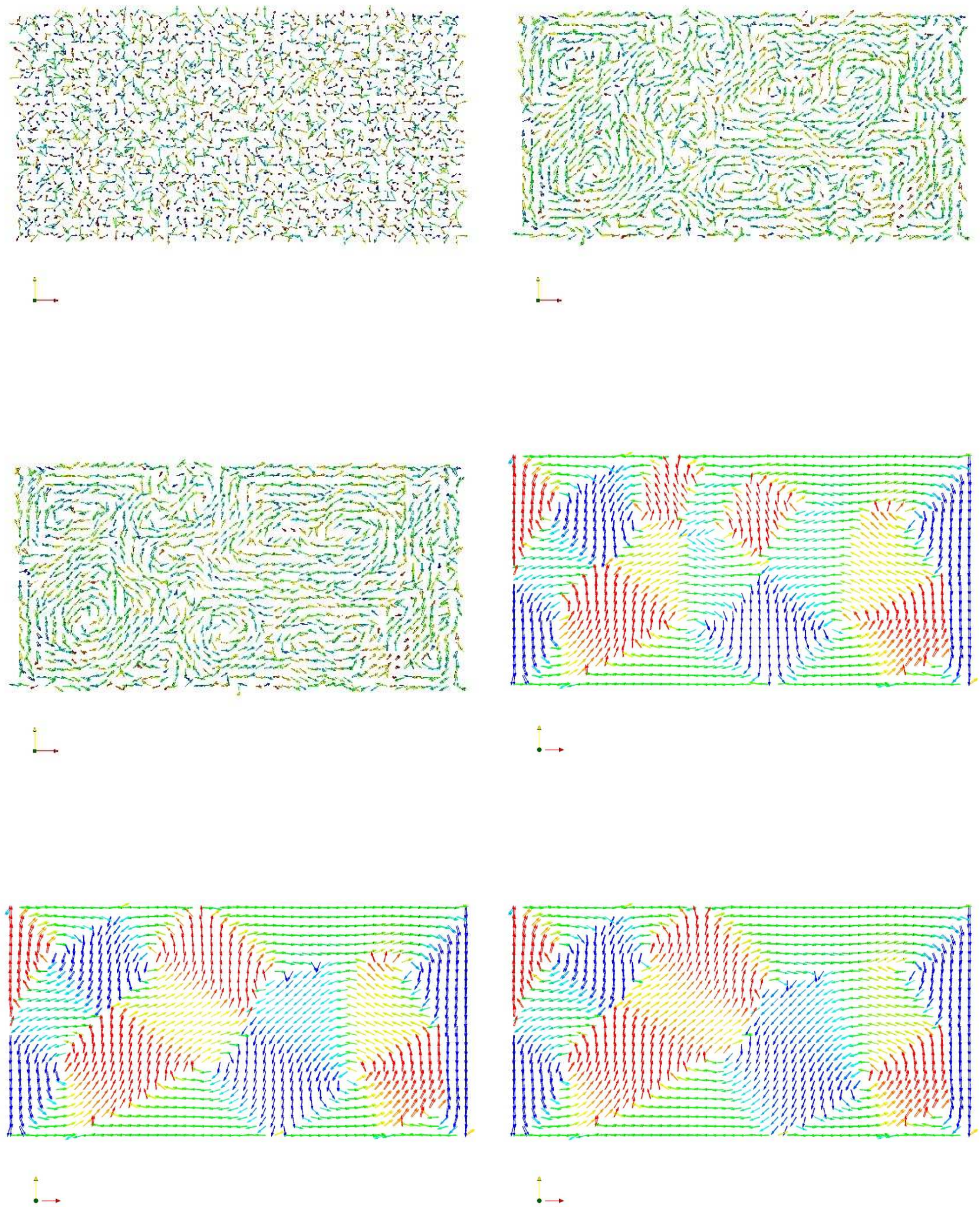

FIGURE 8. Example 5.2: Magnetization at times $t = 0, 100, 200, 2500, 5000, 8000$ (from left to right, from top to bottom).

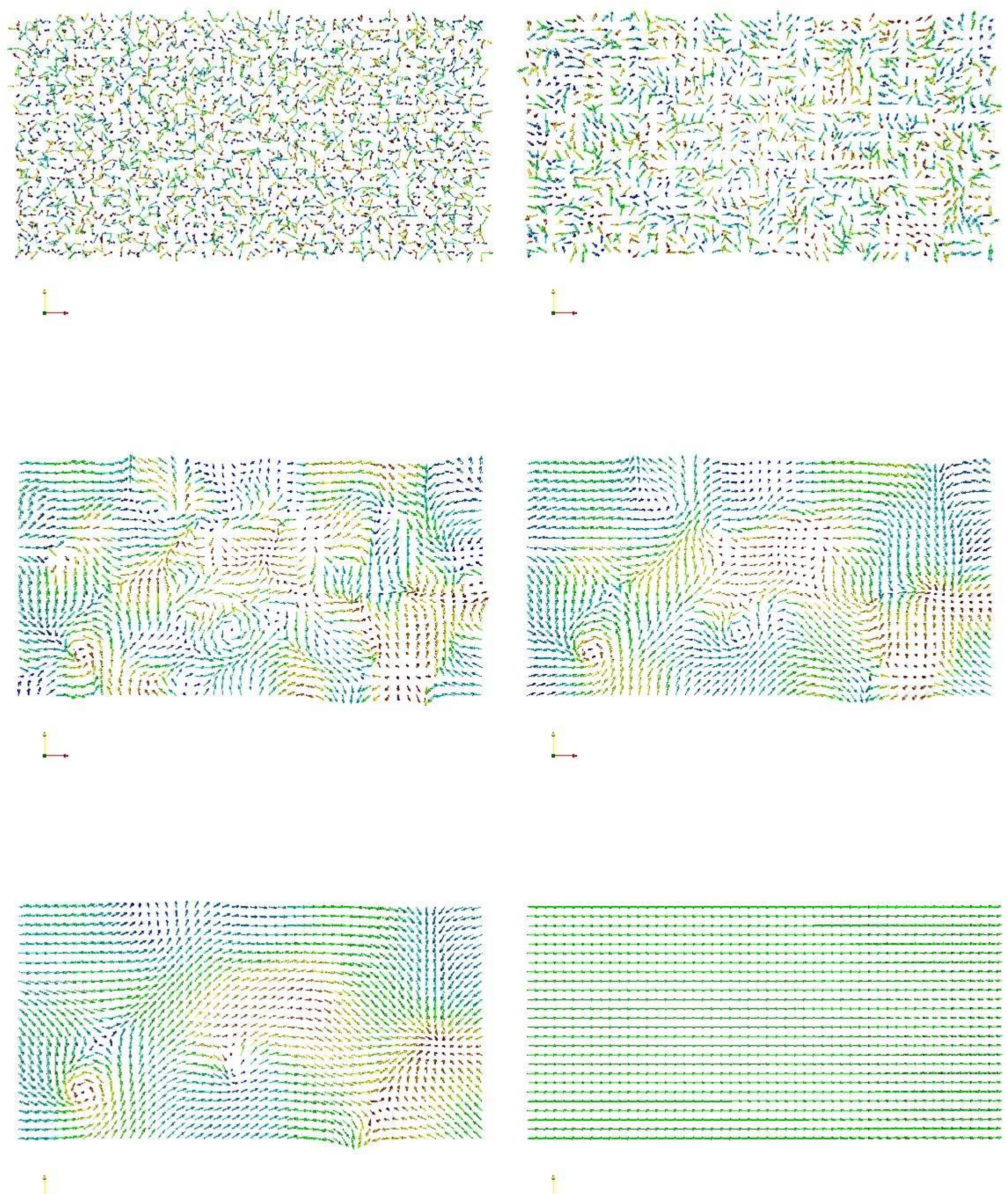

FIGURE 9. Example 5.2: Magnetization without the magnetic field at times $t = 0, 10, 50, 100, 200, 2500$ (from left to right, from top to bottom).

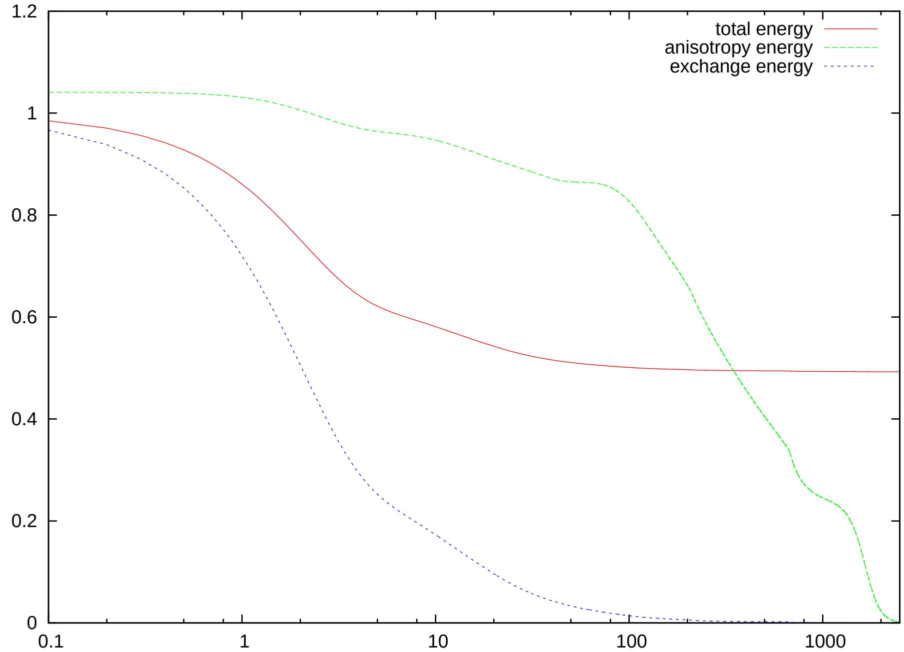

FIGURE 10. Example 5.2: Evolution of the energies, $\log(t) \mapsto \mathcal{E}_T(t)/11$, $\mathcal{E}_{ex}(t)/11$, $\mathcal{E}_{an}(t)/0.04$.

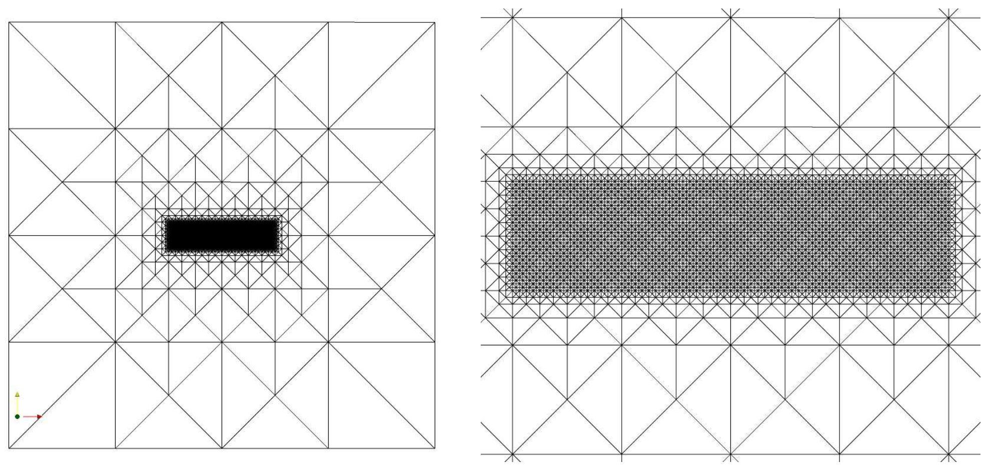

FIGURE 11. Example 5.3: Mesh for the domain Ω at $x_3 = 0$ (left) and zoom at the mesh for the domain ω at $x_3 = 0$ (right).

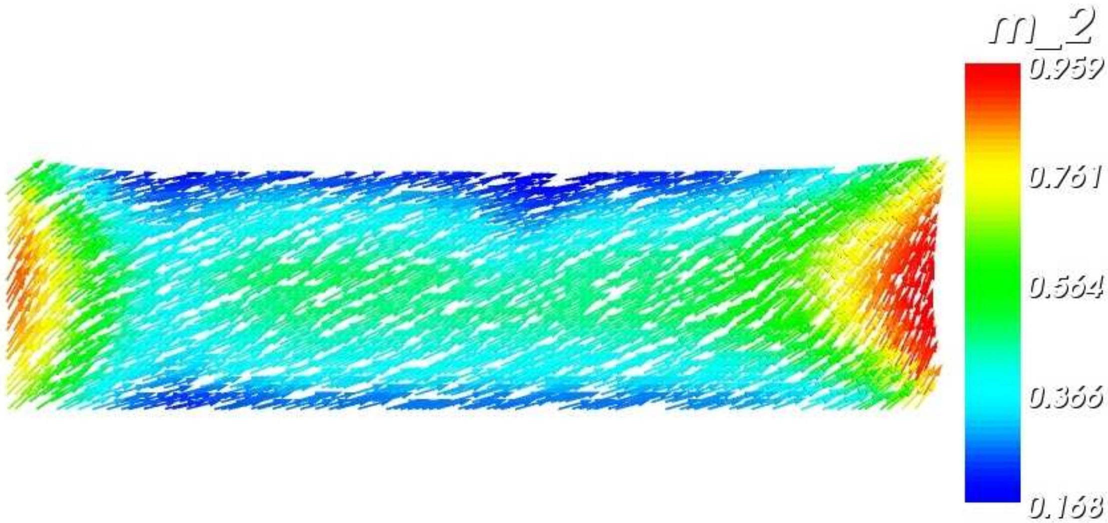

FIGURE 12. Example 5.3: Magnetization at time $t = 300$, near the S-state.

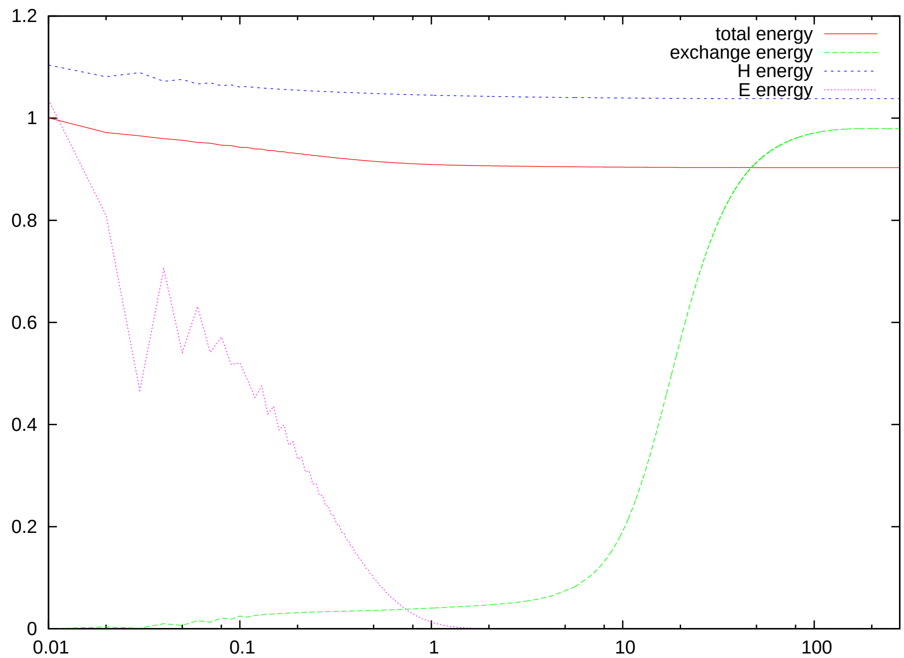

FIGURE 13. Example 5.3: Evolution of the energies, $\log(t) \mapsto \mathcal{E}_T(t)/2.3$, $\mathcal{E}_{ex}(t)/0.0004$, $\mathcal{E}_H(t)/2$, $\mathcal{E}_E(t)/0.09$.